Beyond the Bowel: Extraintestinal Manifestations of Inflammatory Bowel Disease[1]

Jeffrey D. Olpin, MD
Brett P. Sjoberg, MD
Sarah E. Stilwill, MD
Leif E. Jensen, MD, MPH
Maryam Rezvani, MD
Akram M. Shaaban, MBBCh

Abbreviations: ASAS = Assessment of SpondyloArthritis Society, IBD = inflammatory bowel disease, IgG4 = immunoglobulin G4, PSC = primary sclerosing cholangitis, STIR = short inversion time inversion-recovery

RadioGraphics 2017; 37:1135–1160

https://doi.org/10.1148/rg.2017160121

Content Codes: CH GI GU MK

[1]From the Department of Diagnostic Radiology (J.D.O., S.E.S., L.E.J., M.R., A.M.S.), University of Utah, 30 North 1900 East, #1A71, Salt Lake City, UT 84132; and the Department of Diagnostic Radiology, University of Wisconsin, Madison, Wis (B.P.S.). Presented as an education exhibit at the 2015 RSNA Annual Meeting. Received April 25, 2016; revision requested October 14 and received November 22; accepted January 10, 2017. For this journal-based SA-CME activity, the authors, editor, and reviewers have disclosed no relevant relationships. **Address correspondence to** J.D.O. (e-mail: *jeffrey.olpin@hsc.utah.edu*).

SA-CME LEARNING OBJECTIVES

After completing this journal-based SA-CME activity, participants will be able to:

- List the various extraintestinal organ systems that can be affected in the setting of Crohn disease and ulcerative colitis.
- Describe specific extraintestinal disorders that are strongly or loosely associated with IBD.
- Discuss the roles of CT and MR imaging in the evaluation of patients suspected of having extraintestinal manifestations of IBD.

See www.rsna.org/education/search/RG.

Inflammatory bowel disease (IBD) is a chronic, relapsing immune-mediated inflammation of the gastrointestinal tract. IBD includes two major disease entities: Crohn disease and ulcerative colitis. Imaging plays an important role in the diagnosis and surveillance of these complex disorders. Computed tomographic and magnetic resonance enterographic techniques have been refined in recent years to provide a superb means of evaluating the gastrointestinal tract for suspected IBD. Although the intestinal imaging manifestations of IBD have been extensively discussed in the radiology literature, extraintestinal imaging manifestations of IBD have received less attention. Multiple extraintestinal manifestations may be seen in IBD, including those of gastrointestinal (hepatobiliary and pancreatic), genitourinary, musculoskeletal, pulmonary, cardiac, ocular, and dermatologic disorders. Although many associations between IBD and extraintestinal organ systems have been well established, other associations have not been fully elucidated. Some extraintestinal disorders may share a common pathogenesis with IBD. Other extraintestinal disorders may occur as a result of unintended treatment-related complications of IBD. Although extraintestinal disorders within the abdomen and pelvis may be well depicted with cross-sectional enterography, other musculoskeletal and thoracic disorders may be less evident with such examinations and may warrant further investigation with additional imaging examinations or may be readily apparent from the findings at physical examination. Radiologists involved in the interpretation of IBD imaging examinations must be aware of potential extraintestinal manifestations, to provide referring clinicians with an accurate and comprehensive profile of patients with these complex disorders.

Introduction

Inflammatory bowel disease (IBD) is a chronic, relapsing immune-mediated inflammation of the gastrointestinal tract. The two major subtypes of IBD are Crohn disease and ulcerative colitis. Imaging plays an important role in the detection, characterization, and surveillance of IBD. Both computed tomographic (CT) enterography and magnetic resonance (MR) enterography have emerged in recent years as invaluable tools in the assessment of IBD. Although such techniques are optimized for evaluation of the bowel, extraintestinal manifestations of IBD are being increasingly recognized at cross-sectional imaging. Multiple extraintestinal manifestations of IBD can be seen with imaging examinations optimized for evaluation of the bowel, including manifestations of hepatobiliary, pancreatic, genitourinary, musculoskeletal, pulmonary, and cardiac disorders.

Extraintestinal manifestations are estimated to occur in 21%–47% of patients with IBD (1). The pathogenesis of most extraintestinal manifestations is not well understood. However, with the advent

TEACHING POINTS

- Multiple extraintestinal manifestations of IBD can be seen with imaging examinations optimized for evaluation of the bowel, including manifestations of hepatobiliary, pancreatic, genitourinary, musculoskeletal, pulmonary, and cardiac disorders.
- Extraintestinal manifestations involving the skin, eyes, and joints usually parallel the degree of intestinal inflammation, but other extraintestinal manifestations involving gastrointestinal (hepatobiliary) and cardiothoracic disorders typically do not correspond to the degree of intestinal inflammation.
- PSC is a chronic biliary disorder that represents the most common hepatobiliary manifestation of IBD.
- Enterourinary fistulas represent the most common urinary manifestation of IBD, with colovesical fistulas being the most common type of fistula.
- IBD-related spondyloarthropathy is a type of seronegative spondyloarthropathy, a category of inflammatory arthropathy that includes idiopathic ankylosing spondylitis, psoriatic arthritis, reactive arthritis, and undifferentiated spondyloarthropathy.

of genomewide association studies, substantial advances have been made in the genetic basis of IBD in recent years. Specifically, 99 susceptibility loci or genes (71 for Crohn disease and 47 for ulcerative colitis) have been published to date (2). Most important, the findings of these studies have provided deeper insight into shared pathways between IBD and related extraintestinal disorders, pathways that continue to evolve (Table 1).

Extraintestinal manifestations of IBD involve multiple organ systems throughout the body (Table 1). Extraintestinal manifestations involving the skin, eyes, and joints usually parallel the degree of intestinal inflammation, but other extraintestinal manifestations involving gastrointestinal (hepatobiliary) and cardiothoracic disorders typically do not correspond to the degree of intestinal inflammation (1).

Although optimal assessment of the bowel is of utmost importance when performing and interpreting CT and MR enterographic examinations, crucial extraintestinal manifestations of IBD may be inadvertently ignored (Fig 1). Clinical radiologists must be aware of potential extraintestinal manifestations, to provide referring clinicians with an accurate and comprehensive assessment of patients with these complex disorders. Additional imaging examinations may even be warranted if a clinically suspected extraintestinal manifestation is not adequately evaluated with an examination optimized for bowel evaluation.

Gastrointestinal (Hepatobiliary and Pancreatic) Manifestations of IBD

Hepatobiliary and pancreatic disorders account for some of the most common extraintestinal manifestations encountered in the setting of IBD.

Table 1: Extraintestinal Manifestations of IBD

Group	Extraintestinal Manifestations
Gastrointestinal	Primary sclerosing cholangitis (PSC)
	PSC–autoimmune hepatitis overlap syndrome
	Drug-induced hepatitis
	Hepatic steatosis
	Hepatic abscess
	Portal vein thrombosis
	Pancreatitis
	Immunoglobulin G4 (IgG4)–associated cholangitis*
	Primary biliary cirrhosis*
	Cholelithiasis*
	Autoimmune pancreatitis*
Urinary	Enterourinary fistulas
	Obstructive uropathy
	Nephrolithiasis*
Musculoskeletal	IBD-related arthropathy
	Osteoporosis
	Osteonecrosis
	Osteomyelitis or abscess
	Hypertrophic osteoarthropathy
Pulmonary	Large airways disease
	Pneumonia*
Cardiac	Congestive heart failure*
Ocular or orbital	Conjunctivitis
	Episcleritis
	Orbital pseudotumor*
Cutaneous	Enterocutaneous fistulas
	Pyoderma gangrenosum
	Erythema nodusum

*Conditions that have an equivocal or indirect association with IBD.

Although the links between IBD and many hepatobiliary disorders have been well elucidated, other associations remain more elusive (Table 2).

Primary Sclerosing Cholangitis

PSC is a chronic biliary disorder that represents the most common hepatobiliary manifestation of IBD (3). The association between PSC and IBD was first described in 1965 by Smith and Loe (4).

PSC is typically diagnosed in patients between the 3rd and 5th decades of life, with a 2:1 male predominance (5). PSC appears to be most common in white populations, with an increased prevalence in North America and Europe. It is estimated that 70%–80% of patients with PSC have concomitant IBD, and 1.4%–7.5% of patients with IBD will ultimately develop PSC (6). Of these patients, 85%–95% have ulcerative colitis, and the remaining patients have Crohn colitis or Crohn ileocolitis (7). Patients with both

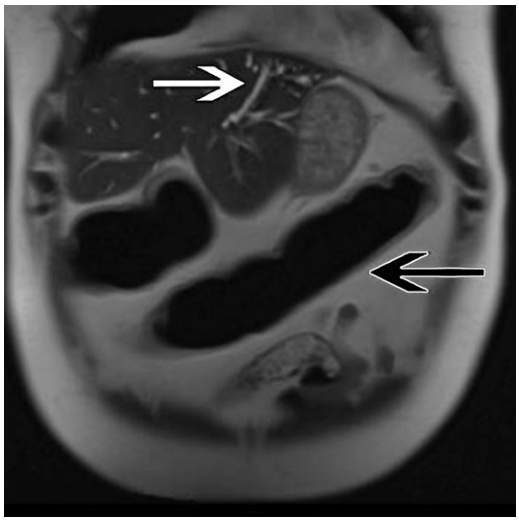

Figure 1. Ulcerative colitis in a 31-year-old man with clinically unsuspected PSC. Coronal T2-weighted MR enterographic image shows a segment of featureless transverse colon with loss of haustral markings consistent with ulcerative colitis (black arrow). Abnormally dilated bile ducts (white arrow) are depicted within the left hepatic lobe, findings consistent with concomitant PSC.

Table 2: Hepatobiliary and Pancreatic Manifestations of IBD

Disorder Group	Hepatobiliary and Pancreatic Manifestations
Disorders that may share a common pathogenesis with IBD	PSC, small-duct PSC, autoimmune hepatitis, idiopathic pancreatitis, IgG4-associated cholangitis
Disorders that parallel the pathophysiology of an underlying IBD	Gallstones, portal vein thrombosis, hepatic abscess
Disorders that may occur as a complication of IBD treatment	Drug-induced hepatitis, reactivation of hepatitis B, drug-induced pancreatitis, hepatosplenic T-cell lymphoma
Disorders possibly associated with IBD	Autoimmune pancreatitis, hepatic steatosis, primary biliary cirrhosis

PSC and IBD tend to exhibit a pattern of IBD progression that is distinctly different from that of patients who have IBD without associated PSC. Hence, the term *PSC-IBD* was coined by investigators from the Mayo group to classify these patients with both PSC and IBD as having a separate clinical entity (8).

The sequence of IBD diagnosis and PSC diagnosis varies. For some patients, the onset of ulcerative colitis may occur years after a diagnosis of PSC. However, new onset of PSC may not be diagnosed until years after a diagnosis of ulcerative colitis (9). An increased risk for colonic dysplasia or colon cancer exists in patients with the PSC-IBD combination. The findings from a meta-analysis suggest that the presence of PSC was shown to be an independent risk factor for the development of colorectal dysplasia or colon cancer in patients with ulcerative colitis, with an odds ratio of 4.79 (10).

The prevalence of PSC appears to be directly related to the degree of small bowel and colonic involvement in patients with IBD. The subset of IBD patients with extensive colonic involvement or pancolitis is more likely to have coexisting PSC, with an estimated prevalence of 5.5%; patients with a distal colitis have an estimated prevalence of PSC of only 0.5% (7). In addition, no cases have been reported of PSC occurring in IBD patients in whom the disease is strictly confined to the small bowel (7). The presence of concomitant PSC may also be associated with the extent and severity of ulcerative colitis. Several investigators have suggested that IBD in the setting of PSC is characterized by a higher incidence of rectal sparing, backwash ileitis, pancolitis, and colitis-associated neoplasia, with an overall poorer survival rate (8).

PSC is characterized by progressive inflammation, obliterative fibrosis, and destruction of both the intrahepatic biliary tree and the extrahepatic biliary tree, leading to the development of biliary fibrosis, cirrhosis, and eventual hepatic failure (1).

Although the clinical overlap between ulcerative colitis and cholestatic liver disease has long been established, the pathogenesis of PSC remains somewhat elusive to date. It is generally accepted that PSC and IBD share a common pathogenesis (1). The association of PSC with IBD and other autoimmune disorders suggests that genetic and immunologic factors are crucial in the development of PSC-IBD. Indeed, several autoimmune disorders, such as type 1 diabetes mellitus and

Graves disease, are common in patients with PSC-IBD (11). Strong evidence supports the belief that host immunity plays an important role in the pathogenesis of PSC (1). Other investigators have suggested that microbiologic mechanisms may partially account for the link between PSC and IBD (12). "Leaky gut" may likewise play a role in the pathogenesis of PSC (13).

Patients with PSC may exhibit symptoms of jaundice, pruritus, fatigue, abdominal pain, and weight loss at presentation. However, only 10%–15% of patients exhibit symptoms at the time of diagnosis, while 60% of patients develop symptoms with time (14). Patients presenting with PSC typically have abnormal results of liver function tests. Specifically, elevated alkaline phosphatase levels are commonly seen, which are indicative of cholestasis. A number of autoantibodies can be detected in the setting of PSC, including antinuclear antibodies, anti–smooth muscle antibodies, and perinuclear antineutrophil cytoplasmic antibodies (pANCA). However, these antibodies are fairly nonspecific, and the role of antibody detection in patients with PSC is not well established.

Imaging plays a substantial role in the detection, characterization, and surveillance of PSC. Endoscopic retrograde cholangiopancreatography is traditionally considered the reference standard in the evaluation of PSC. Hallmark features of PSC at cholangiography include multifocal "beaded" strictures of both the intrahepatic and extrahepatic bile ducts, with intervening sites of dilated and normal-caliber ducts. Strictures may vary in length from approximately 1–2 mm to several centimeters. A dominant stricture has been described as marked dilatation of the duct upstream from a tight, long stricture (stricture diameter <1.5 mm in the common bile duct or <1 mm in the left or right main duct). A dominant stricture that either persists or progresses with time should raise concern for cholangiocarcinoma. Abrupt biliary termination, or "pruning," of the biliary tree may occur with time. Intraluminal filling defects may occur in the bile ducts and are generally indicative of biliary calculi when the defects are between 2 and 5 mm in diameter. However, larger nodular defects should raise concern for cholangiocarcinoma. Although endoscopic retrograde cholangiopancreatography can be both diagnostic and therapeutic in the assessment of PSC, the invasive nature of the examination carries the risk of inherent morbidities such as cholangitis and pancreatitis.

Ultrasonography (US) of the liver may be used in some centers as a screening tool in patients with abnormal results of liver function tests. Although US may be used to detect biliary dilatation, biliary wall thickening, and bile duct stones in the setting of PSC, sonographic interrogation of PSC is generally very limited. Scant information has been published regarding the role of US in PSC screening.

CT plays little role in the detection of early PSC, because depiction of the biliary tree with CT is inherently limited. Findings may include alternating areas of stenosis and dilatation of the bile ducts. Abnormal arborization of the bile ducts has been described, in which branching ducts appear discontinuous on sequential images. Abnormal biliary wall thickening and enhancement may likewise be seen. Imaging findings of chronic PSC are generally better depicted with CT, including peripheral hepatic atrophy and central hepatic hypertrophy with a diffusely macronodular liver contour.

MR imaging has emerged in recent years as the most effective noninvasive technique for the evaluation of both early and late stages of PSC (Fig 2). In particular, for MR cholangiopancreatography, a heavily T2-weighted coronal pulse sequence is used, which provides superior noninvasive depiction of the biliary tree. In 2006, one group of investigators reported that MR cholangiopancreatography had a sensitivity of 80%, a specificity of 87%, and a diagnostic accuracy of 83% in the diagnosis of PSC, values only slightly inferior to those for endoscopic retrograde cholangiopancreatography (15). MR cholangiopancreatographic findings of PSC include multifocal, or "beaded," strictures of the intrahepatic and extrahepatic bile ducts, with alternating sites of biliary dilatation (Fig 3). On MR cholangiopancreatographic images, excessive numbers of peripheral ducts have been described as a result of peripheral downstream strictures. Hepatolithiasis and choledocholithiasis are optimally depicted as signal voids on MR images obtained with all pulse sequences (Fig 4). Contrast material–enhanced T1-weighted MR images may optimally demonstrate biliary wall thickening and hyperenhancement. Findings of chronic PSC are readily depicted on MR images as peripheral hepatic atrophy and central hypertrophy with a diffusely macronodular liver contour (Fig 5). T2-weighted MR images may demonstrate areas of patchy hyperintensity, which are indicative of parenchymal edema and inflammation. In patients with chronic PSC, confluent fibrosis may be seen as wedge-shaped areas of parenchymal volume loss that appear hypointense on T1-weighted MR images and hyperintense on T2-weighted and delayed contrast-enhanced T1-weighted MR images.

PSC–Autoimmune Hepatitis Overlap Syndrome

An overlap between PSC and autoimmune hepatitis has been described in patients with IBD, particu-

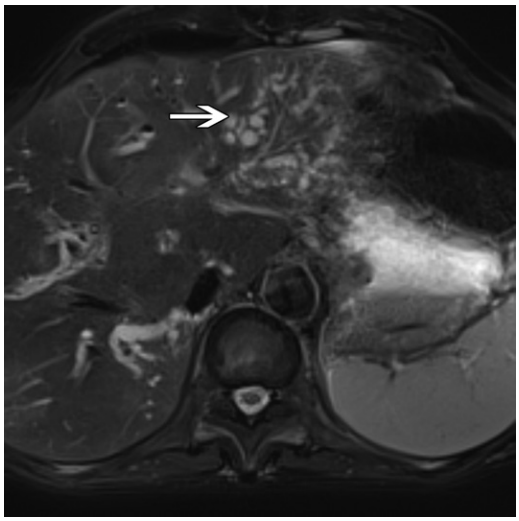

Figure 2. PSC in a 46-year-old woman. Axial T2-weighted fat-saturated MR image shows diffuse contour irregularity throughout the liver. Diffusely irregular calibers of the bile ducts are noted throughout the liver, with predominant involvement of the lateral segment of the left hepatic lobe (arrow).

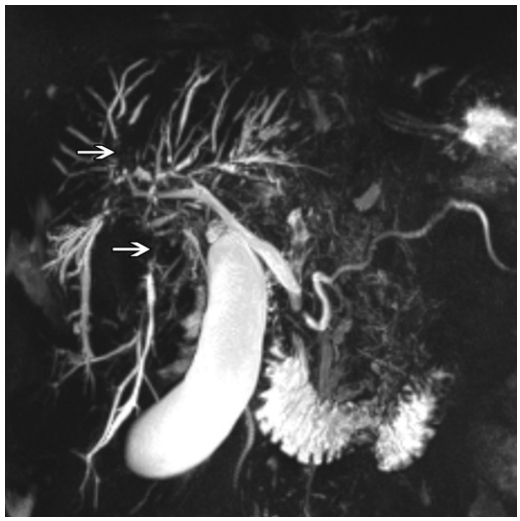

Figure 3. PSC in a 37-year-old woman. Coronal thick-slab MR cholangiopancreatographic image shows diffuse irregularity of the bile ducts, with areas of stenosis (arrows) and dilatation throughout the liver.

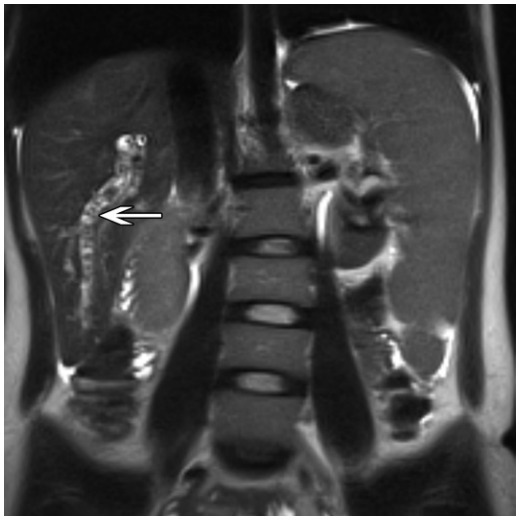

Figure 4. Biliary lithiasis in a 39-year-old man with PSC. Coronal T2-weighted MR image shows diffuse dilatation of a bile duct within the right hepatic lobe. Multiple filling defects (arrow) are noted throughout the duct, findings consistent with biliary lithiasis.

larly in those patients with ulcerative colitis. Multiple case reports have been published of patients with IBD in whom autoimmune hepatitis was definitively diagnosed and who later developed histologic evidence of PSC (16). However, the diagnosis is difficult to establish because the clinical and imaging features of both disease processes overlap, and diagnostic criteria have not been firmly established to date. The diagnosis of overlap syndrome is suspected when a definite diagnosis of autoimmune hepatitis is established on the basis of the International Autoimmune Hepatitis Group criteria, including demographics, laboratory markers, and liver histologic findings (17). The diagnosis should be suspected in IBD patients with typical imaging findings of PSC in conjunction with imaging features of autoimmune hepatitis: cirrhotic liver morphology with widened hepatic fissures, liver surface nodularity, caudate enlargement, periportal fibrosis, and signs of portal hypertension (18).

Cholangiocarcinoma

A dreaded complication of PSC is the development of cholangiocarcinoma, a devastating malignancy with an extremely poor prognosis. Although cholangiocarcinoma may not be a direct result of IBD, the strong association between PSC and cholangiocarcinoma has been well established in the literature (1). It is imperative that radiologists interpreting imaging examinations in PSC patients maintain a high index of suspicion for the presence of an underlying cholangiocarcinoma.

Cholangiocarcinoma is the second most common primary hepatic tumor after hepatocellular carcinoma. The 5-year survival rate of individuals with cholangiocarcinoma is between 5% and 10%. PSC is one of the most common risk factors for cholangiocarcinoma in Western countries (19). Cholangiocarcinoma in PSC patients tends to manifest earlier than cholangiocarcinomas that occur sporadically (20). Patients with PSC are at a significantly increased risk for developing cholangiocarcinoma, with a lifetime incidence of 5%–15% (21). Although patients with PSC may benefit from liver transplantation, those with underlying cholangiocarcinoma are generally ineligible for transplantation, because patients with underlying malignancy have a poor prognosis. Therefore, it is of vital

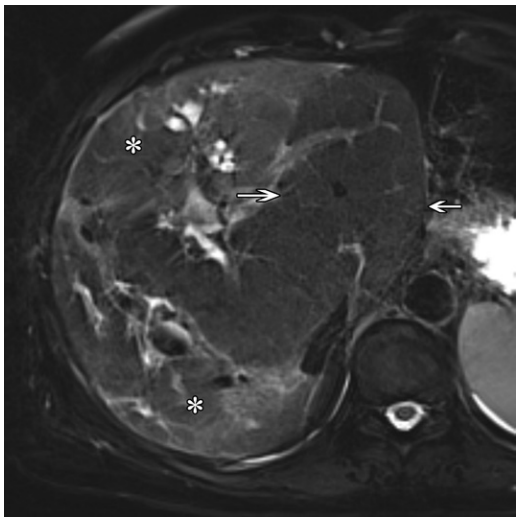

Figure 5. Chronic PSC in a 57-year-old man. Axial T2-weighted fat-saturated MR image shows a diffusely irregular macrolobular liver contour with central or caudate hypertrophy (arrows) and peripheral atrophy (*). Scattered areas of mildly increased signal intensity are noted throughout the peripheral liver, findings consistent with diffuse fibrosis.

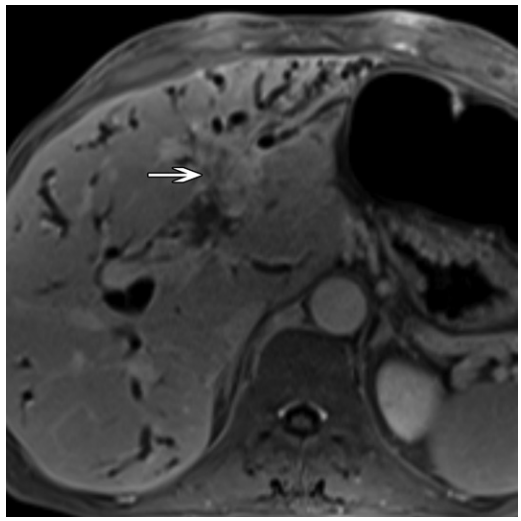

Figure 6. Hilar cholangiocarcinoma in a 62-year-old man with chronic PSC. Axial contrast-enhanced T1-weighted MR image shows an enhancing mass arising from the central left intrahepatic bile duct (arrow). Scattered biliary dilatation is noted throughout the liver, with predominant involvement of the lateral segment of the left hepatic lobe upstream from the enhancing mass.

importance to establish the diagnosis of cholangiocarcinoma in the setting of PSC.

Although various classification schemes for cholangiocarcinoma have been proposed, an anatomic classification is generally the most widely adopted. Peripheral cholangiocarcinomas, or those tumors that occur proximal to secondary biliary radicles, account for 10% of cholangiocarcinomas. Peripheral cholangiocarcinomas are typically large and tend to manifest late in the course of the disease. Perihilar cholangiocarcinomas account for 50% of cholangiocarcinomas and are often subcategorized according to the Bismuth-Corlette classification for the purpose of optimizing surgical planning (Fig 6). Klatskin tumors are a subtype of perihilar cholangiocarcinomas that occur at the confluence of the main right and left bile ducts within the porta hepatis. Distal cholangiocarcinomas are extrahepatic lesions, generally involving the distal common bile duct, that account for the remaining 40% of cholangiocarcinomas.

The diagnosis of cholangiocarcinoma is generally established with a combination of clinical, laboratory, and imaging findings. Unfortunately, the imaging findings of PSC and cholangiocarcinoma frequently overlap, and current imaging techniques generally fail to detect cholangiocarcinoma in the setting of PSC until most tumors are fairly advanced and inoperable.

Cholangiocarcinoma can manifest with a wide spectrum of imaging findings. Common CT and MR imaging features of cholangiocarcinoma include focal thickening of the bile duct wall, focal biliary dilatation out of proportion to the dilatation seen in the background of PSC, capsular retraction, and portal vein invasion. MR imaging has generally been regarded as the reference standard imaging technique for the characterization and staging of cholangiocarcinoma. Advantages of MR imaging include superior soft-tissue contrast resolution, which allows for optimal tumor depiction and superior assessment of the bile ducts with MR cholangiopancreatographic techniques (22). Contrast-enhanced T1-weighted MR imaging is generally superior to CT in the detection of small hilar tumors and periductal tumor infiltration. Mass-forming lesions often demonstrate delayed enhancement because of the presence of concomitant fibrous stroma.

Drug-induced Hepatitis

Although the previously described hepatobiliary disorders share a common pathogenesis with IBD, therapy with a number of the drugs used in the treatment of IBD can result in iatrogenic hepatotoxic effects. A number of drugs have been implicated, including thiopurines, methotrexate, sulfasalazine, cyclosporine, and biologic agents such as infliximab, adalimumab, and certolizumab. Manifestations of hepatotoxicity include elevated results of liver function tests and clinical influenza-like symptoms that generally resolve after discontinuation of therapy with the drugs. In some instances, percutaneous liver biopsy may be warranted to establish the presence of drug-induced hepatitis. Although there are no specific guidelines for the use of methotrexate in IBD patients, the American Academy of Dermatology

Figure 7. Acute hepatitis in a 47-year-old woman with chronic Crohn disease. Transverse gray-scale US image of the liver shows diffusely hypoechoic parenchyma with increased echogenicity of the portal triads (arrow), the "starry sky" appearance, predominantly involving the left hepatic lobe.

Figure 8. Hepatic steatosis in a 42-year-old man with PSC. Axial T1-weighted opposed-phase MR image shows ill-defined areas of decreased signal intensity (arrow) within the central liver, findings consistent with hepatic steatosis.

has recommended surveillance with liver biopsies for patients with psoriasis and rheumatoid arthritis who are being treated with methotrexate (23).

Although imaging findings of drug-induced hepatitis are often subtle and nonspecific, several features of nonspecific acute hepatitis can be seen at imaging, including hepatomegaly, periportal edema, diffuse or focal fatty infiltration, and gallbladder wall thickening (24). At US, the classic so-called starry sky appearance has been widely described in the setting of acute hepatitis and is due to the increased echogenicity of portal venous walls (Fig 7) (25). A rare complication of therapy with azathioprine (a thiopurine) is the development of hepatic veno-occlusive disease, which has been described in the literature (26). Imaging features of veno-occlusive disease include hepatosplenomegaly, ascites, and periportal and gallbladder wall edema. US findings include hepatofugal portal venous flow and elevated values for the arterial resistive index (>0.75) at Doppler US interrogation.

Hepatic Steatosis

Hepatic steatosis, or fatty liver, is the most common hepatobiliary complication of IBD (27). One group of investigators reported that fatty liver was seen in 35% of 511 patients with IBD (28). However, tremendous variability has been reported in the prevalence of fatty liver, ranging from 13% to 100% in published studies (1). A correlation between the degree of fatty liver infiltration and the severity of colitis has been shown in patients with ulcerative colitis (29). Although the etiology of fatty liver development in the setting of IBD remains somewhat elusive, factors such as chronic malnutrition, protein loss, and corticosteroid therapy are likely contributing factors (1).

Sonographic features of fatty liver include increased parenchymal echogenicity with increased attenuation of the ultrasound beam. At CT, fatty liver is optimally assessed on nonenhanced images as decreased attenuation of the liver compared with the spleen. The attenuation of the liver is inversely proportional to the degree of underlying steatosis. On contrast-enhanced CT images, attenuation measurements are less reliable than on nonenhanced CT images. However, most experts agree that liver steatosis is present when the attenuation of the background liver parenchyma is more than 35 HU less than that of the spleen on portal venous phase images (30). MR imaging findings of fatty liver are readily assessed at T1-weighted chemical shift imaging. The liver parenchyma demonstrates decreased signal intensity on out-of-phase images relative to the in-phase images in the presence of hepatic steatosis (Fig 8) (31). The degree of the decrease in the signal intensity on out-of-phase images is likewise proportional to the severity of hepatic steatosis.

Hepatic Abscess

Patients with IBD have a slightly higher incidence of pyogenic liver abscesses than the general population (27). Investigators have suggested that the loss of integrity of the normal mucosal barrier in the bowel may result in microbial invasion of the mesenteric veins, with resultant seeding of the liver (1). Concomitant portal vein thrombosis may likewise occur in the setting of infectious

Figure 9. Hepatic abscess in a 48-year-old man with PSC and ulcerative colitis. Axial contrast-enhanced CT image shows diffusely dilated biliary ducts within the anterior segment of the right hepatic lobe (black arrow). A focal area of decreased attenuation (*) is seen within the caudate lobe, a finding consistent with abscess. Vague scattered areas of decreased attenuation (white arrow) are seen within the posterior segment of the right hepatic lobe, findings consistent with a developing abscess.

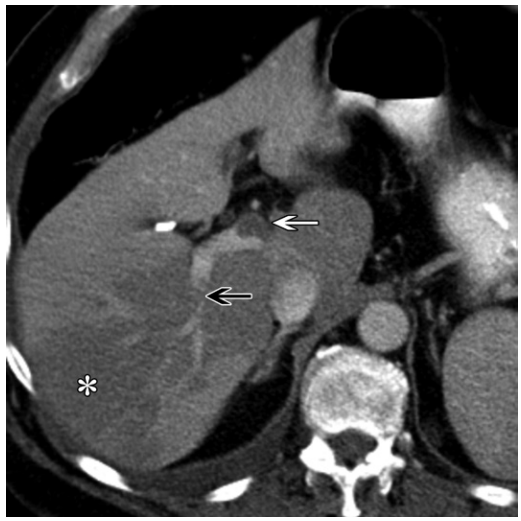

Figure 10. Portal vein thrombosis in a 59-year-old woman with chronic ulcerative colitis. Axial contrast-enhanced CT image shows partially obstructive thrombus (white arrow) within the main portal vein, with poorly organized thrombus (black arrow) in the posterior branch of the right portal vein. An area of geographic decreased attenuation (*) is seen within the posterior segment of the right hepatic lobe, a finding consistent with segmental hepatic steatosis from altered lipid metabolism in the setting of segmental portal vein thrombosis.

portal pyelophlebitis. Single or multiple liver abscesses have been reported as an initial manifestation of Crohn disease (32).

US often serves as an initial screening tool for a patient suspected of having a liver abscess. US features include spherical or ovoid intrahepatic lesions that are anechoic in 50% of individuals, hyperechoic in 25% of individuals, and hypoechoic in the remaining 25% of individuals. Although early abscesses are usually poorly marginated and hyperechoic, more mature abscesses become progressively distinct and less hyperechoic (33). Internal septa or fluid-fluid levels may be seen in a pyogenic abscess. Brightly hyperechoic foci with posterior artifact may be seen in the setting of gas-forming organisms. CT and MR imaging findings of a pyogenic abscess include a unilocular or multilocular mass with central nonenhancing debris and peripheral rim or capsular enhancement, the so-called target sign (34). Small abscesses may coalesce into a larger abscess with time, the so-called cluster sign (Fig 9) (35).

Portal Vein Thrombosis

The portal vein is a common site of thrombosis in patients with IBD (27). Although portal vein thrombosis is a rare complication of IBD, the incidence of portal vein thrombosis in patients with IBD appears to be higher than that of the general population, likely because of coagulation abnormalities from underlying chronic bowel inflammation or infectious pyelophlebitis, as previously discussed (36). Patients with IBD have increased platelet counts, fibrinogen levels, and factor V and VIII levels, as well as decreased antithrombin III levels, all of which can increase the risk of thrombosis. Portal vein thrombosis occurs more frequently in the setting of recent abdominal surgery in patients with IBD (37). A high incidence of portal vein thrombosis has been reported after restorative proctocolectomy in patients with ulcerative colitis. Baker et al (38) reported CT evidence of portal venous thrombi in 45% of patients who had recently undergone ileal pouch–anal anastomosis for ulcerative colitis.

US generally serves as the initial imaging modality for suspected portal vein thrombosis. Imaging features include a hyperechoic or anechoic portal venous filling defect in the acute phase that becomes progressively isoechoic with time. Lack of flow or abnormal waveforms within the portal vein are generally evident at color Doppler US interrogation (39). CT findings of portal venous thrombosis include low-attenuation thrombus within the portal vein that is most apparent at portal venous phase imaging (Fig 10). Arterial phase images may demonstrate a transient area of increased attenuation within an affected hepatic segment that is due to arterioportal shunting, otherwise known as a transient hepatic attenuation difference. Although MR imaging is generally not the modality of choice, a hyperintense filling defect may be seen within the portal veins on T1- and T2-weighted

Figure 11. Acute pancreatitis in a 57-year-old woman with chronic Crohn disease. Axial contrast-enhanced CT image shows diffuse edematous enlargement of the entire pancreas (*), with peripancreatic fat stranding (arrows).

MR images in the setting of portal vein thrombosis (39). Arterial phase images may likewise demonstrate a hepatic segment of hyperenhancement from arterioportal shunting, otherwise known as a transient hepatic intensity difference.

Pancreatitis

Patients with IBD are at increased risk of developing acute pancreatitis and chronic pancreatitis. However, most cases of IBD-associated pancreatitis are clinically silent. Hyperamylasemia or exocrine pancreatic insufficiency may be the only manifestation of pancreatitis in these individuals (40). However, an elevation of the serum amylase level is not always indicative of pancreatitis. Abnormal serum amylase levels have been reported in 5.8%–15.8% of patients with IBD (41). The clinical importance of elevated pancreatic enzyme levels in the asymptomatic patient with IBD is not entirely clear.

Several mechanisms have been proposed for the development of IBD-associated acute pancreatitis. Acute pancreatitis may be secondary to *(a)* gallstones, *(b)* Crohn disease affecting the duodenum, with resultant papillary dysfunction, or *(c)* Crohn disease–associated granulomatous inflammation of the pancreas (42). Acute drug-induced pancreatitis has been reported after administration of IBD medications such as 5-aminosalicylates, corticosteroids, azathioprine, or 6-mercaptopurine, although the reported incidence is low (43). Acute pancreatitis likewise occurs in the setting of PSC with sclerosis of the pancreatic ducts as well as the bile ducts, otherwise known as "sclerosing pancreatitis" (44).

CT imaging features of acute pancreatitis include edematous pancreatic enlargement, often with loss of the normal fatty pancreatic lobulation. Peripancreatic fat stranding, edema, and free fluid are also commonly seen in acute pancreatitis (Fig 11). Parenchymal necrosis may occur in the setting of necrotizing pancreatitis, which is optimally depicted on contrast-enhanced images (45). MR imaging findings of acute pancreatitis may demonstrate pancreatic enlargement with increased signal intensity throughout the pancreas on T2-weighted MR images, findings consistent with pancreatic edema. T1-weighted contrast-enhanced MR images may show areas of pancreatic nonenhancement, which are consistent with necrotizing pancreatitis. MR cholangiopancreatographic techniques provide a superior noninvasive means of assessing the integrity of the pancreatic duct (46). Although US plays little role in the evaluation of acute pancreatitis, an enlarged hypoechoic pancreas with adjacent free fluid may be seen.

The relationship between chronic pancreatitis and IBD was first described in 1950 by Ball et al (47), who found that 46 (53%) of 86 patients with ulcerative colitis demonstrated chronic interstitial pancreatitis at postmortem examination. As with acute pancreatitis, it appears that in most IBD patients with chronic pancreatitis, the condition is clinically silent (1). An autopsy study of 39 IBD patients showed pancreatic fibrosis in 38% of patients, although none had previous clinical or laboratory evidence of pancreatitis (48). The etiology of IBD-associated chronic pancreatitis remains elusive. A common autoimmune pathway has been suggested, because autoantibodies against the pancreatic antigens in the pancreatic juice were detected in blood samples of 40% of patients with Crohn disease and 4% of patients with ulcerative colitis (49).

CT and MR imaging findings of chronic pancreatitis include irregular pancreatic ductal dilatation with intervening strictures. Pancreatic parenchymal and intraductal calcifications are virtually pathognomonic for chronic pancreatitis and are

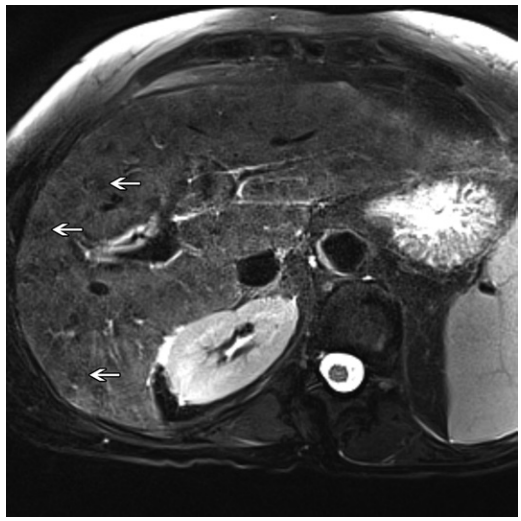

Figure 12. Primary biliary cirrhosis in a 68-year-old man with chronic ulcerative colitis. Axial T2-weighted fat-saturated MR image shows mild hepatomegaly with diffuse parenchymal nodularity. Scattered areas of decreased signal intensity (arrows) surround the portal veins, findings consistent with the periportal halo sign.

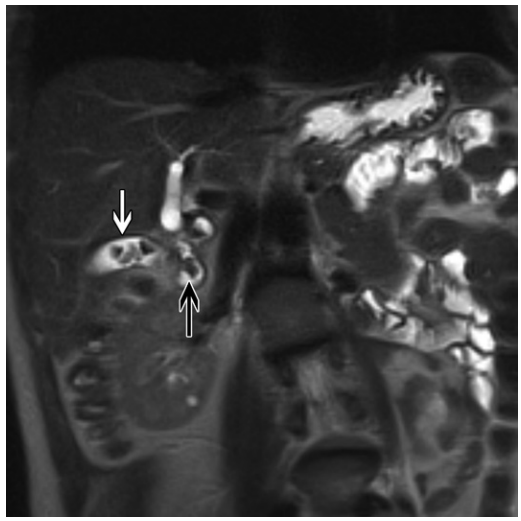

Figure 13. Cholelithiasis in a 44-year-old woman with Crohn disease. Coronal T2-weighted fat-saturated MR image shows multiple gallstones (white arrow) in a partially contracted gallbladder, with stones extending into a dilated cystic duct (black arrow).

optimally detected with CT. Diffuse pancreatic parenchymal atrophy is also commonly seen, which is often more apparent in the distal body and tail (50). MR imaging is generally more sensitive to early changes of chronic pancreatitis, as evidenced by the loss of the inherent T1-hyperintense signal intensity in the pancreatic parenchyma (51).

Diseases Loosely Associated with IBD

IgG4-associated Cholangitis.—IgG4-associated cholangitis has been well described in patients with IgG4-associated disease, with the hallmark entity consisting of autoimmune pancreatitis. Although a strong association between IBD and PSC has been extensively documented, some investigators have suggested a link between ulcerative colitis and IgG4-associated cholangitis. Although imaging features of IgG4-associated cholangitis may be similar to those of PSC, IgG4-associated cholangitis appears to be a histologically and pathogenetically distinct entity. The distinction is important, because IgG4-associated cholangitis typically shows a dramatic response to corticosteroid therapy, in contrast to PSC (52).

Primary Biliary Cirrhosis.—Primary biliary cirrhosis is an autoimmune liver disease characterized by chronic inflammatory destruction and obliteration of the intrahepatic bile ducts, with infiltration of lymphocytes and plasma cells into the portal tract (53). An association between primary biliary cirrhosis and IBD has been suggested in the literature but has not been widely recognized to date (53). Imaging features of primary biliary cirrhosis include hepatomegaly, lacelike fibrosis, and regenerative nodules. With advanced primary biliary cirrhosis, signs of portal hypertension are frequently seen, including varices, ascites, and splenomegaly. Although primary biliary cirrhosis is often difficult to differentiate from other forms of cirrhosis, lymphadenopathy is more commonly seen in the setting of primary biliary cirrhosis. Wenzel et al (54) described the so-called periportal halo sign on MR images as highly specific for the diagnosis of primary biliary cirrhosis (Fig 12).

Cholelithiasis.—Gallstones are commonly encountered in patients with IBD (Fig 13). Gallstone formation is thought to arise from pathophysiologic changes that parallel the progression of IBD. A strong association between cholelithiasis and Crohn disease has been established, with a reported prevalence between 13% and 34% (1). The association between cholelithiasis and

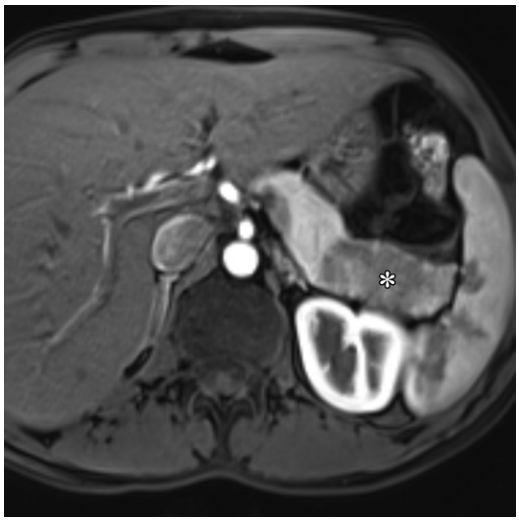

Figure 14. Autoimmune pancreatitis in a 54-year-old woman with ulcerative colitis. Axial contrast-enhanced T1-weighted fat-saturated MR image shows diffuse enlargement of the pancreas, with loss of the normal lobular architecture. A sharply marginated area of hypoenhancement (*) involves the distal body and tail of the pancreas, a finding consistent with segmental autoimmune pancreatitis.

ulcerative colitis is controversial, because there appears to be no significantly increased prevalence of gallstones in patients with ulcerative colitis, when compared with the prevalence in the general background population (28).

Autoimmune Pancreatitis.—Some investigators have suggested a link between IBD and autoimmune pancreatitis, although the exact relationship is not entirely clear to date. IBD-associated pancreatitis has been shown to share similar clinical, morphologic, and histologic features as those seen in autoimmune pancreatitis (1). One group of investigators found that 6% of patients with proven autoimmune pancreatitis had a diagnosis of IBD, compared with a prevalence of 0.4%–0.5% of the general population (55).

Imaging features of autoimmune pancreatitis include diffuse or focal enlargement of the pancreatic parenchyma, with loss of the normal lobular pancreatic architecture. The affected portions of the pancreas have also been described as "sausage-like" in morphologic structure (Fig 14). A low-attenuation or hypointense halo or capsule surrounding the pancreas may also be seen. The pancreatic duct may be diffusely narrowed in affected segments of the pancreas (56).

Urinary Manifestations of IBD

Various urinary complications can be seen in the setting of IBD, with the vast majority occurring in patients with Crohn disease. The incidence of urinary complications in patients with Crohn disease has been reported to be 4%–23% (57). Such complications are more common among individuals with severe or long-standing disease. Urinary complications may be either directly or indirectly related to the underlying disease process. Imaging plays a role in the evaluation of the most common genitourinary manifestations, such as enterourinary fistulas, obstructive uropathy, and nephrolithiasis.

Enterourinary Fistulas

Enterourinary fistulas represent the most common urinary manifestation of IBD, with colovesical fistulas being the most common type of fistula. Although fistulas confined to the gastrointestinal tract are fairly common in Crohn disease, fistulas between the gastrointestinal tract and the urinary system are far less-common yet serious complications, occurring in 2%–3.5% of patients with Crohn disease (57). Most patients are in their 4th or 5th decade with a well-established history of IBD. There is a male predominance ranging from 1.4/1 to 7/1, which is likely due to the protective interposition of the uterus and adnexa between the bowel and bladder in women (58). Crohn disease is the third most common cause of enterourinary fistulas after diverticulitis and cancer. Most enterourinary fistulas involve communication between the sigmoid colon or terminal ileum and the bladder (58). Less-common fistulas include rectovesical, rectourethral, anourethral, colovaginal, urethrocutaneous, vesicocutaneous, and enteroadnexal fistulas (Fig 15). At physical examination, the typical findings of an enterourinary fistula include fever, abdominal tenderness, and a palpable mass. Pneumaturia, fecaluria, and urorrhea (rectal passage of urine) are uncommon, albeit pathognomonic signs of an enterourinary fistula. A vast majority of affected patients present with urinary tract infections, most frequently with *Escherichia coli* or polymicrobial infections. Indeed, clinicians involved in the treatment of patients with Crohn disease who have recurrent urinary tract infections should have a high index of suspicion for an enterourinary fistula.

Although cystography and fluoroscopic barium studies were once considered the imaging

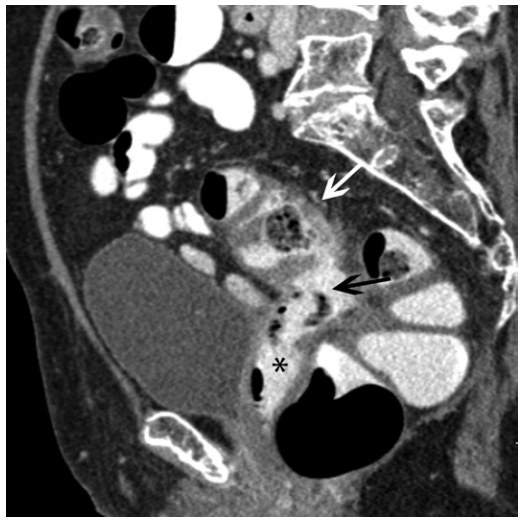

Figure 15. Colovaginal fistula in a 54-year-old woman with Crohn disease. Sagittal contrast-enhanced CT image obtained after administration of oral contrast material shows a large communication (black arrow) between the colon (white arrow) and the contrast material–filled vagina (*).

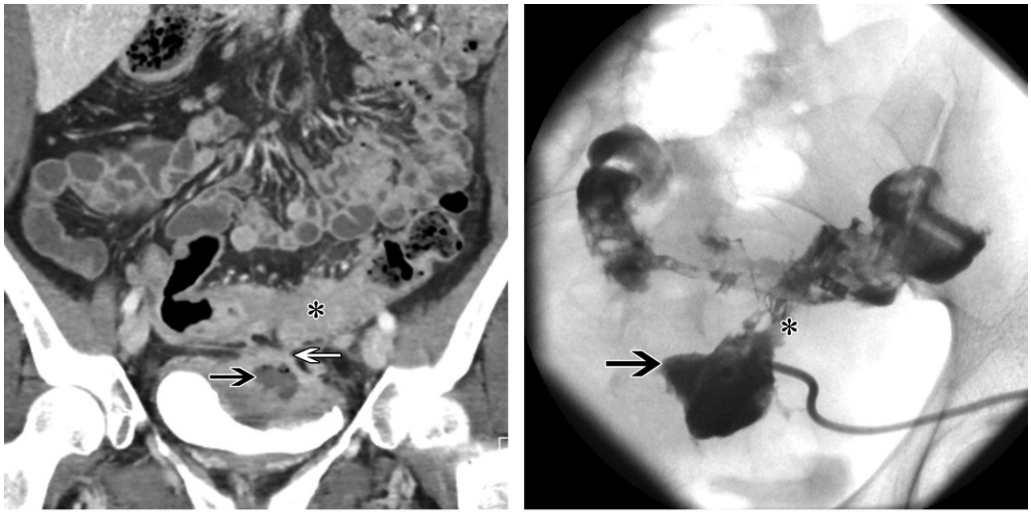

a. **b.**

Figure 16. Colovesical fistula in a 47-year-old woman with Crohn disease. **(a)** Coronal contrast-enhanced CT image shows a fistula (white arrow) between a segment of diffusely thickened sigmoid colon (*) and the urinary bladder wall. The dome of the bladder is markedly thickened and contains an intramural abscess (black arrow). **(b)** Fluoroscopic spot image from an abscessogram obtained after percutaneous drainage of an intramural bladder dome abscess shows opacification of the intramural abscess cavity (arrow), with persistent fistulous communication (*) with the adjacent sigmoid colon.

examinations of choice for the detection of an enterourinary fistula, CT is now the reference standard, because it provides an optimal assessment of the entire collecting system and gastrointestinal tract (Fig 16). Imaging findings of an enterourinary fistula include intraluminal gas within the bladder, apposition of thickened bowel and bladder walls, a paravesical mass, and the presence of enteric contrast material within the bladder (59).

MR imaging has emerged in recent years as an attractive alternative to CT for the assessment of IBD, particularly in those individuals at risk for high radiation exposure. MR imaging is particularly effective in the evaluation for a suspected fistula between the bowel and the female genital tract, given the inherently superior multiplanar capability and excellent soft-tissue resolution of MR imaging (Fig 17).

Obstructive Uropathy

Acalculous obstructive uropathy is a frequently overlooked and underestimated urologic complication of Crohn disease, occurring in 1.9%–6% of patients with Crohn disease (57). Hydroureteronephrosis is caused by transmural bowel inflammation that results in ureteral compression, fibrosis, or encasement that almost invariably involves the right collecting system. Obstructive uropathy most frequently occurs in the setting of active ileocolic disease causing fistulization (60). Even mild hydronephrosis should not be

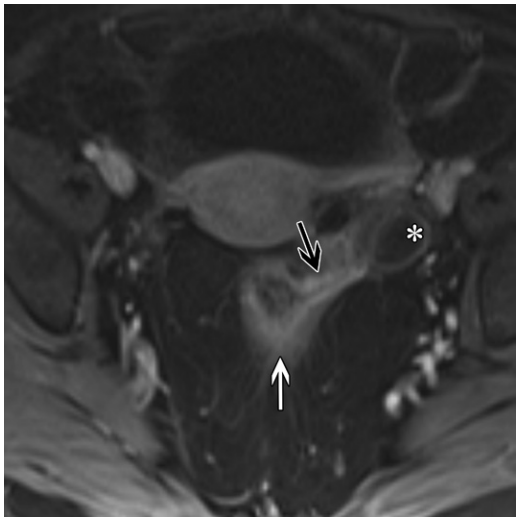

Figure 17. Rectal-adnexal fistula in a 39-year-old woman with Crohn disease. Axial contrast-enhanced T1-weighted MR image shows diffuse thickening and mucosal enhancement of the rectum (white arrow). A fistula (black arrow) extends from the rectum to the adjacent left adnexal tissue, which resulted in a hydrosalpinx (*).

Figure 18. Acalculous obstructive uropathy in a 46-year-old woman with chronic Crohn disease. Oblique coronal contrast-enhanced CT image shows moderate hydronephrosis of the right kidney (white arrow) and proximal ureter (not shown). No obstructing nephrolithiasis is shown. Note the diffuse thickening and enhancement of the terminal ileum and cecum (black arrow), resulting in regional dilatation of the distal ileum.

overlooked at imaging, because irreversible renal damage can occur, often in relatively young patients. Although US may serve as a screening tool for suspected obstructive uropathy, CT and MR imaging are better able to provide a more comprehensive assessment of the entire collecting system and gastrointestinal tract (Fig 18). Most patients with significant obstructive uropathy will require surgical ureterolysis and ileocolic resection.

Nephrolithiasis

Patients with IBD are 10–100 times more likely to develop nephrolithiasis than general hospital patients, with a reported incidence of 12% in patients with Crohn disease (57). Adults are at higher risk than children, as are patients with Crohn disease compared with patients with ulcerative colitis (61). In patients with Crohn disease, stones are more common in those with ileocolic disease than in those with isolated ileal or colonic disease alone, and the stones more commonly involve the right collecting system (62).

Kidney stones in patients with IBD are composed primarily of calcium oxalate or uric acid. The pathophysiology of calcium oxalate stone formation in the setting of IBD is complex, relating to altered intestinal hyperabsorption of oxalate (61). Urate stones in IBD form as a result of increased intestinal fluid and bicarbonate losses, which result in concentrated acidic urine (63).

Imaging plays a crucial role in suspected nephrolithiasis. Renal US can be used to assess for renal calculi and hydronephrosis with a high degree of accuracy. An additional advantage of US is the lack of ionizing radiation, a crucial factor when evaluating the typically young patients with IBD who may require many radiologic examinations during their lifetime. CT of the abdomen and pelvis without administration of intravenous contrast material remains the examination of choice for suspected nephrolithiasis, because CT provides a more comprehensive overview of the urinary tract (64). In addition, CT provides optimal assessment of the gastrointestinal tract to exclude potential acute intestinal complications in the setting of underlying IBD. MR urography has likewise emerged in recent years as an attractive alternative for the evaluation of suspected nephrolithiasis when use of ionizing radiation is contraindicated (65).

Musculoskeletal Manifestations of IBD

Musculoskeletal manifestations of IBD are numerous, with musculoskeletal system–related pain occurring in up to 53% of patients (66). IBD arthropathy has both peripheral and axial sites of disease involvement, with articular involvement present in approximately 30% of IBD patients (67). Additional rheumatologic complications of IBD include osteoporosis, septic arthritis or osteomyelitis, soft-tissue infection, secondary hypertrophic osteoarthropathy, and osteonecrosis (a complication of steroid therapy).

IBD-related Spondyloarthropathy

IBD-related spondyloarthropathy is a type of seronegative spondyloarthropathy, a category of inflammatory arthropathy that includes idiopathic ankylosing spondylitis, psoriatic arthritis, reactive arthritis, and undifferentiated spondyloarthropathy. The clinical and imaging findings of these inflammatory processes are often indistinguishable; however, imaging findings are important for diagnosis. IBD-related spondyloarthropathy is divided into axial and peripheral arthropathy. Axial manifestations include sacroiliitis, inflammatory back pain, and spondylitis. Peripheral arthritis includes a self-limiting nondeforming arthritis that waxes and wanes with bowel flares.

Molecular and biochemical links between intestinal and synovial inflammation ("gut-synovial axis") have been well described in the literature, involving both underlying cell-mediated and humeral immune responses. Environmental and host factors likely trigger an inflammatory pathway in genetically predisposed individuals (68). The end result likely includes activated intestinal lymphocytes adhering to inflamed synovial vessels by means of multiple adhesion molecules and receptors (69). Implicated alleles and genetic associations are well characterized and beyond the scope of this article. Of note, subclinical bowel inflammation has been identified in all subtypes of spondyloarthropathy (70) and likely plays a role in the apparent joint inflammation. In IBD-related spondyloarthropathy, peripheral and axial arthritis may precede or coincide with the onset of intestinal symptoms.

Peripheral Arthropathy

Peripheral arthritis is present in 2.8%–31% of IBD patients (67), with predominantly asymmetric joint involvement classically affecting the knees and ankles. Disease presence and symptoms mirror gut activity. Peripheral arthropathy is more commonly seen in patients with Crohn disease, especially in the setting of Crohn disease with colonic involvement (69). Orchard et al (71) first divided peripheral IBD-related arthropathy into two categories. Type 1 is the most common, with pauciarticular large-joint arthropathy involving less than five joints. Type 1 tends to be acute in onset, asymmetric, and self-limiting, lasting less than 10 weeks. Permanent structural joint damage is uncommon. Large weight-bearing joints are most commonly affected. Symptoms are strongly associated with IBD flares and other extraintestinal IBD manifestations. Type 2 peripheral IBD-related arthropathy is less common and typically symmetric in distribution, involving more than five joints (72). Symptoms can persist for months to years, with erosions and structural deformity more common in the chronic type 2 form (68). Metacarpophalangeal joints are the most commonly involved site of disease in the type 2 form. Unlike type 1, polyarticular arthropathy runs a course independent of inflammatory bowel activity and is less associated with other extraintestinal manifestations.

Common imaging findings of peripheral IBD-related arthropathy include dactylitis, enthesitis, and periarticular osteopenia. Because most peripheral arthropathy in patients with IBD is the pauciarticular and self-limiting variety, radiographs are usually normal. When present, radiographic findings are nonspecific and include periarticular osteopenia, soft-tissue swelling, and joint effusions. Joint destruction is rare, but erosions or osteophytes can be present (Fig 19a).

Enthesitis is a common finding in all of the seronegative spondyloarthropathies and has been described in 6%–50% of patients in IBD population studies (67). Enthesitis occurs as focal inflammation at a tendon, ligament, or joint capsule at a bone attachment site. Early radiographic findings include *(a)* osteopenia that is due to hyperemia and, later, *(b)* bone proliferation or ossification at the enthesis, with spur formation. MR imaging findings reflect this focal inflammation and include marrow edema at the enthesis on MR images obtained with fluid-sensitive sequences, as well as enhancement on contrast-enhanced T1-weighted MR images. US can play a role in monitoring treatment response, including the presence of tendon edema, tendon calcifications, hyperemia, peritendonitis, and osseous erosions (73). Common sites of tendon involvement in patients with spondyloarthropathy include the Achilles tendon and plantar fascia insertions on the calcaneus, as well as the patellar tendon insertion on the tibial tubercle (74). The most common sites of enthesitis in axial spondyloarthropathy include the interosseous ligaments of the sacroiliac joints, as well as annular ligament–vertebral body endplate attachments in the spine. Costovertebral, costosternal, and manubriocostal enthesitis can be the source of chest pain and poor inspiration.

Figure 19. Chronic bilateral sacroiliitis in the setting of IBD in two different patients. **(a)** Sacroiliitis in a 50-year-old man with ankylosing spondylitis: Anteroposterior pelvic radiograph shows fusion of the sacroiliac joints and severe secondary peripheral osteoarthritis at the hip joints (white arrow), as well as chronic spine findings, including the "dagger spine sign" (black arrow), which represents ossification of the supraspinous and interspinous ligaments. **(b, c)** Sacroiliitis in a 65-year-old woman with Crohn disease who had undergone proctocolectomy. **(b)** Anteroposterior pelvic radiograph shows evidence of the prior bowel surgery (white arrow), with fusion of the sacroiliac joints (black arrow). **(c)** Axial contrast-enhanced CT image of the same patient shown in **b** obtained 3 years later shows dilatation of the small bowel, with an enterocutaneous fistula (white arrow). The bilateral sacroiliac joints (black arrow) are fused. (Case and Figure 19b and 19c courtesy of Loren G. Longenecker, MD, University of California-San Diego, La Jolla, Calif.)

a.

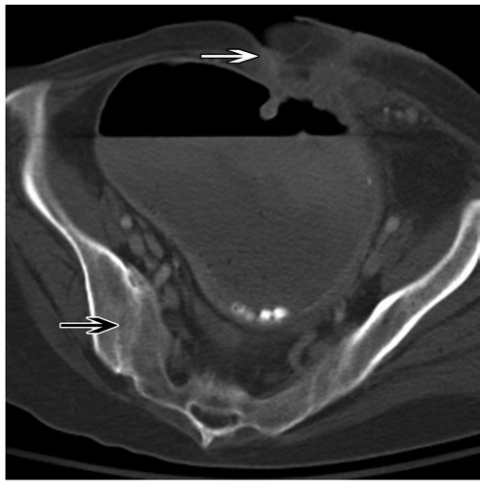

c.

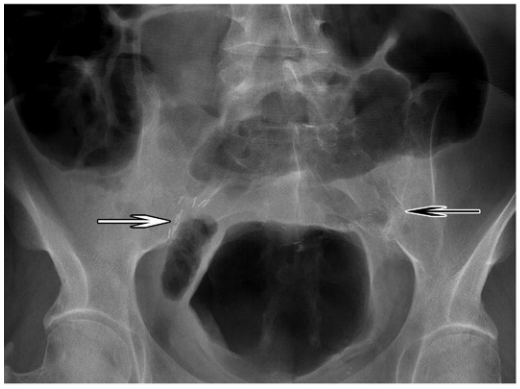

b.

Dactylitis, or "sausage digit," is a classic finding of psoriatic spondyloarthropathy but has also been described in 2%–4% of IBD patients (69). Manifesting as pain and diffuse swelling of a digit, dactylitis occurs when joint inflammation extends beyond the capsule, extending in the adjacent soft tissue and the coursing flexor tendon sheaths. Findings are usually clinically evident, with the most common MR imaging and US findings including flexor tendon tenosynovitis and joint synovitis (75).

Axial Arthropathy

Clinical and imaging findings of axial arthropathy in IBD-related spondyloarthropathy classically include inflammatory back pain, sacroiliitis, and ankylosing spondylitis. The course of axial arthropathy is independent of IBD activity, and bowel surgery does not alter the course of sacroiliitis or IBD-related spondylitis (76). Imaging plays a crucial role in the diagnosis of sacroiliitis and spondylitis. Axial manifestations of IBD-related spondyloarthropathy frequently precede the diagnosis of IBD by several years, making the identification of early manifestations crucial for early diagnosis and treatment of IBD.

The reported prevalence of isolated sacroiliitis in IBD varies widely from 16% to 46% (73). These patients have imaging features of sacroiliitis without meeting the clinical criteria for ankylosing spondylitis. Classic diagnostic criteria for ankylosing spondylitis and spondyloarthropathy, such as the modified New York criteria (77), the Amor criteria (78), and the criteria of the European Spondyloarthropathy Study Group (79), include radiographic findings as an important component. Unfortunately, radiographic and CT imaging findings most commonly show sequelae of long-standing chronic inflammation, with limited ability to diagnose active or acute inflammation. Several years may pass before radiographic findings become evident in a symptomatic patient. As detailed by Navallas et al (80) in their review of spondyloarthropathy-associated sacroiliitis, the increased use of MR imaging has allowed for earlier and more accurate detection of active or acute inflammation, allowing for treatment before the onset of structural damage.

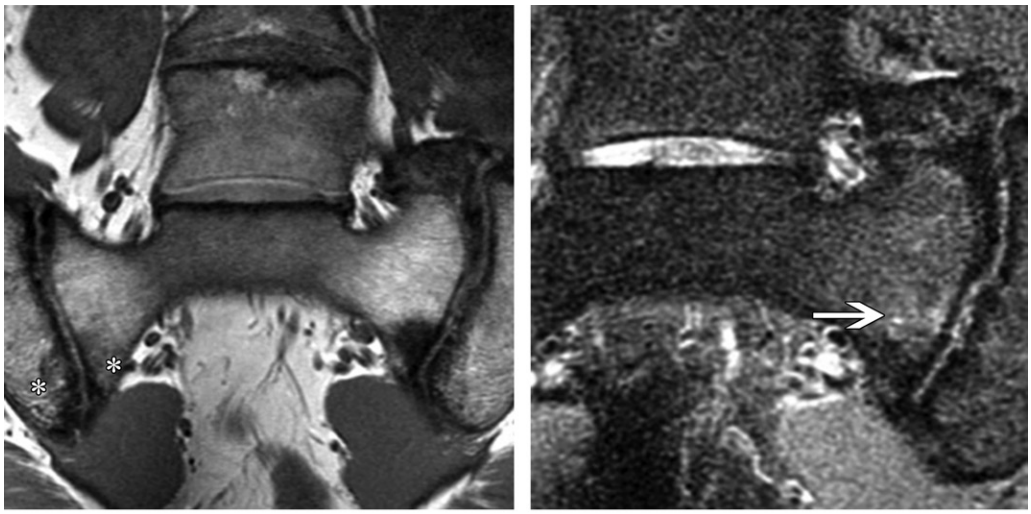

a. b.

Figure 20. Acute inflammation in a 54-year-old woman with chronic sacroiliitis. Coronal T1-weighted **(a)** and STIR **(b)** MR images through the sacroiliac joints show irregularity along the articular margins (* on **a**) with subchondral sclerosis and edema (arrow on **b**), findings consistent with acute on chronic inflammation.

Findings of sacroiliitis are classically bilateral and symmetric but may be unilateral or asymmetric early in the disease process. Erosive changes begin along the distal one-third synovial portion of the joint, as well as the iliac articular margin where the hyaline cartilage is thinner (80). Radiographic and CT findings include a spectrum ranging from erosions to sclerosis and eventual ankylosis. The modified New York criteria (77) include a five-grade scale ranging from a grade of 0 (normal) to 4 (ankylosis) when describing radiographic findings of sacroiliitis, which range from subtle joint space irregularity, to erosions and sclerosis, and eventual ankyloses (Fig 19b). Anteroposterior radiographic technique is usually sufficient, sparing the radiation exposure and expense of specific sacroiliac joint views (81). Inclusion of the hip joints is important, because their involvement is common in spondyloarthropathy and is strongly associated with spinal involvement (80). CT demonstrates similar findings but with better detail and less interobserver variability (Fig 19c).

Whereas CT images and radiographs demonstrate the sequelae of long-standing or chronic inflammation, MR imaging is able to detect acute and early inflammatory changes. Patients with active sacroiliitis at MR imaging may take up to 3–7 years to develop definite radiographic evidence of sacroiliitis (82). Therefore, new diagnostic criteria for the diagnosis of axial spondyloarthropathy have been developed on the basis of MR imaging.

The Assessment of SpondyloArthritis Society (ASAS) Outcome Measures in Rheumatology MR imaging group identified MR imaging findings of sacroiliitis best categorized as either active inflammatory lesions or structural damage lesions (82).

Active inflammatory lesions of the sacroiliac joints include bone marrow edema or osteitis, synovitis, enthesitis, and capsulitis. Subchondral bone marrow edema is hyperintense on short inversion time inversion-recovery (STIR) or fat-saturated T2-weighted MR images and demonstrates correlative hypointensity on T1-weighted MR images. Marrow edema may be associated with erosions and sclerosis (Fig 20). Hyperenhancement of the involved bone on contrast-enhanced T1-weighted fat-saturated MR images reflects increased vascularity and is termed *osteitis*. Synovitis manifests as enhancement of the synovium on contrast-enhanced T1-weighted fat-saturated MR images; note that use of fluid-sensitive sequences alone is unable to allow differentiation of joint fluid from synovitis. Enthesitis of the interosseous ligaments demonstrates hyperintensity on STIR or fat-saturated T2-weighted MR images and contrast-enhanced T1-weighted fat-saturated MR images. The abnormal signal intensity may extend to the adjacent bone marrow and soft tissues. Capsulitis is similar in appearance to synovitis, but signal intensity abnormalities occur at the anterior and posterior capsule. The differential diagnosis for the previously mentioned findings includes septic sacroiliitis; however, infection is more likely to cross anatomic borders and involve the adjacent soft tissues (83). It is important to note that sacroiliac joint osteoarthritis can also mimic inflammatory sacroiliitis, with scattered areas of marrow edema and osteophytes along both sides of the sacroiliac joints.

Structural damage lesions of the sacroiliac joints are the sequelae of chronic sacroiliitis and include subchondral sclerosis, erosions, fat deposition, and bone bridging or ankylosis. Areas of subchondral sclerosis appear as areas of low signal intensity with all pulse sequences, without correlative enhancement on contrast-enhanced images. Because small areas of sclerosis along the sacroiliac joints can be normal, subchondral sclerosis in the setting of sacroiliitis and spondyloarthropathy should extend at least 5 mm from the joint space. Erosions appear at the joint margins and are hypointense on T1-weighted MR images, with associated hyperintensity on STIR MR images. Use of T2-weighted gradient-echo and T1-weighted fat-saturated sequences may increase the sensitivity for identifying erosions. Coalescing erosions can manifest as apparent widening of the joint (pseudowidening). Periarticular fat deposition secondary to (chronic) inflammation manifests as hyperintensity on T1-weighted MR images, with bone bridging or ankylosis occurring late in the development of sacroiliitis and manifesting as low signal intensity with use of all pulse sequences. Hyperintensity on T1-weighted MR images representing fatty marrow may surround the bridging bone.

As defined by the ASAS Outcome Measures in Rheumatology MR imaging group, the new ASAS criteria for axial spondyloarthropathies include inflammation on MR images compatible with sacroiliitis (82). A "positive" MR imaging examination must demonstrate active inflammatory lesions, including marrow edema or osteitis in a subchondral or periarticular distribution typical of spondyloarthropathy. The presence of synovitis, enthesitis, or capsulitis without associated bone marrow edema or osteitis is not sufficient for diagnosis. For abnormal marrow signal intensity to qualify as active inflammation, the abnormality should be present on at least two consecutive sections. One section is sufficient if multiple foci of abnormal signal intensity are present on a single section. Although structural lesions including ankylosis reflect the sequelae of inflammation, these findings alone without acute inflammatory lesions and marrow edema do not meet the criteria for sacroiliitis.

Ankylosing spondylitis is diagnosed when both the clinical criteria for inflammatory back pain and the imaging criteria for sacroiliitis are met. The classic modified New York criteria describe three clinical criteria: *(a)* low back pain and stiffness for more than 3 months, which improves with exercise but is not relieved by rest; *(b)* limitation of motion of the lumbar spine; and *(c)* limitation of chest expansion. The radiologic criterion includes a sacroiliitis grade of 2 or more bilaterally or a sacroiliitis grade of 3–4 unilaterally. Definite ankylosing spondylitis is present if the radiologic criterion is associated with at least one clinical criterion. Other diagnostic criteria exist, and the newer ASAS criteria for axial spondyloarthropathy include MR imaging features of sacroiliitis to allow earlier diagnosis (84). Other criteria use similar principles, and the aforementioned ASAS criteria included MR imaging findings of active sacroiliitis to increase early detection.

Ankylosing spondylitis is present in 1%–16% of IBD patients (67). Of the patients with ankylosing spondylitis, up to 5%–10% were reported to have clinically overt IBD (85). Although the frequency of HLA-B27 antigen in IBD patients is similar to that in the general population, IBD patients with features of ankylosing spondylitis demonstrate positivity for HLA-B27 antigen 25%–78% of the time (69). Ankylosing spondylitis in the setting of IBD-related spondyloarthropathy has no gender predilection.

Imaging findings in ankylosing spondylitis include both sacroiliitis and well-described spine findings (86). The Romanus lesion is the earliest finding in the spine, with anterior and posterior vertebral body endplate irregularities involving the annular ligament attachment site. Although Romanus lesions are visible on radiographs, MR imaging is more sensitive in detecting both early and late Romanus lesions, which appear as hypointensity of the endplate rim on T1-weighted MR images and associated hyperintensity on STIR MR images (Fig 21a, 21b). The abnormal signal intensity represents marrow edema or osteitis, and the localization to the attachment of the anulus fibrosus is consistent with enthesitis. As the disease progresses, the Romanus lesions appear hyperintense on T1-weighted MR images, reflecting postinflammatory fatty bone marrow degeneration. Radiographic "shiny corners" are present after active inflammation has ceased.

Spondylodiscitis, or an Andersson lesion, is a noninfectious inflammatory disk process. One or both vertebral halves demonstrate hemisphere-shaped areas of hyperintensity on STIR MR images and hypointensity on T1-weighted MR images (Fig 21c, 21d). Radiography of these lesions in the late phase of spondyloarthropathy demonstrates central endplate irregularities and erosions. Noninflammatory insufficiency fractures can also occur at the level of the disk or the level of the vertebral body. These fractures will be evident at radiography and MR imaging. Synovial joint arthritis can occur in the facet, costovertebral, and costotransverse joints, with imaging appearances comparable to that of peripheral arthritis, including joint effusion, synovitis, erosions, bone marrow

Figure 21. Axial spondyloarthropathy: spine findings in three different patients. **(a, b)** Spine findings in a 45-year-old man with ulcerative colitis and chronic back pain. Sagittal T1-weighted **(a)** and STIR **(b)** MR images show Romanus lesions at the anterior annular ligament attachment sites; the lesions are depicted as areas of hypointensity on the T1-weighted MR image (arrow on **a**) and areas of hyperintensity on the STIR MR image (arrow on **b**). As the inflammation progresses, these lesions will appear as hyperintense lesions on T1-weighted MR images, with the eventual development of radiographic "shiny corners." **(c, d)** Spine findings in a 29-year-old man with ankylosing spondylitis. Sagittal T1-weighted **(c)** and STIR **(d)** MR images show spondylodiscitis, or an Andersson lesion, with hemispheric hypointensity along the central endplate on the T1-weighted MR image (arrow on **c**) and with hyperintensity on the STIR MR image (arrow on **d**). These lesions are inflammatory and should not be confused with infectious discitis. Note that corner Romanus lesions are also depicted at the anterior and posterior corners. **(e, f)** Spine findings in a 28-year-old man. Anteroposterior **(e)** and sagittal **(f)** radiographs show the classic thin vertical syndesmophytes (white arrow) and fused sacroiliac joints (black arrows on **e**) of ankylosing spondylitis, which is indistinguishable from IBD-related spondyloarthropathy.

edema, and late ankylosis. Enthesitis can occur and is most prominent on images when it involves the interspinal and supraspinal ligaments. Enthesitis manifests as an area of hyperintensity on STIR or contrast-enhanced T1-weighted fat-saturated MR images. The classic syndesmophytes in ankylosing spondylitis occur as bone outgrowths of the anterior vertebral body edge (Fig 21e, 21f). Best depicted with radiography, syndesmophytes can be difficult to detect with MR imaging, demonstrating either low or high signal intensity on STIR MR images, depending on the stage of spondylitis. Ankylosis can occur at either the vertebral edges or center, findings that are thought to represent the sequelae of Romanus lesions and Andersson lesions, respectively.

Other Musculoskeletal Manifestations

Osteoporosis.—Bone demineralization and osteoporosis are commonly described extraintestinal manifestations in patients with IBD and are associated with a 40% greater relative risk of fractures than that of the general population (87). The etiology is multifactorial and may include inflammatory-mediated bone resorption, malabsorption of dietary calcium and magnesium, poor dietary calcium intake because of lactose intolerance, vitamin D deficiency, corticosteroid therapy, reduced physical activity, and decreased serum albumin levels. A detailed literature review by the American Gastroenterological Association (87) demonstrated a modest effect of IBD on bone mineral density, with a 15% overall prevalence of osteoporosis in patients with IBD. The risk of osteoporosis is similar in male and female patients with IBD,

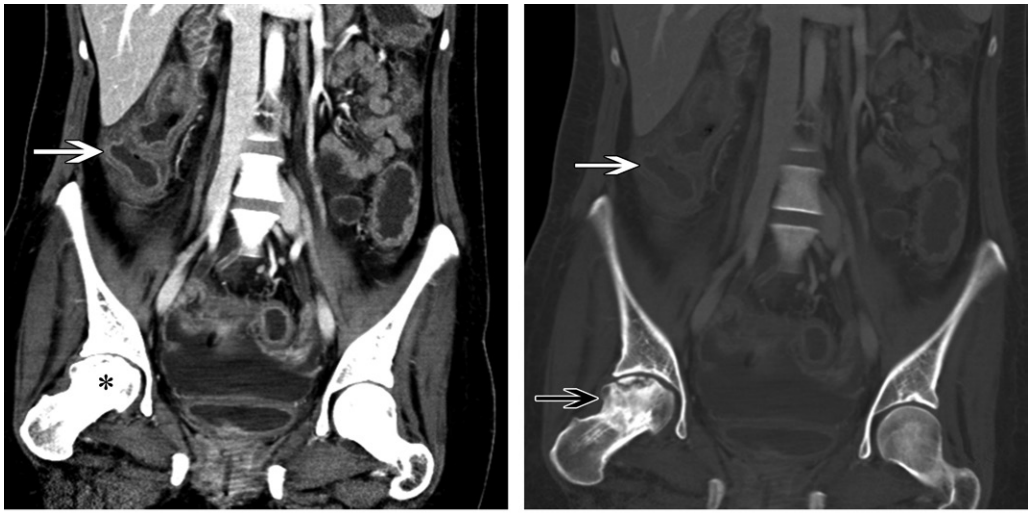

Figure 22. Femoral head avascular necrosis and pancolitis in a 29-year-old woman with ulcerative colitis. **(a)** Coronal contrast-enhanced CT image shows colonic wall thickening and mucosal hyperenhancement (white arrow), findings consistent with pancolitis. Irregularity and flattening of the right femoral head (*) is better evaluated with use of bone windows. **(b)** Coronal CT image (bone window) better shows the sclerosis and deformity of the right femoral head, including a subchondral fracture with femoral head flattening (black arrow), findings consistent with osteonecrosis secondary to corticosteroid therapy. Colonic wall thickening is also depicted (white arrow).

and patients with Crohn disease and ulcerative colitis are of comparable risk. Although corticosteroid therapy is most strongly associated with osteoporosis, this association is confounded by the fact that corticosteroid therapy is associated with active IBD. The results of prior studies describing an increased prevalence of vitamin D deficiency and osteomalacia in patients with IBD were not verified and may not play as important a role in IBD-related osteoporosis.

Osteonecrosis.—Osteonecrosis in the setting of IBD occurs most commonly as a complication of corticosteroid therapy. The femoral head is the most common site, with multifocal involvement seemingly more common when associated with IBD (68). Osteonecrosis in the setting of IBD tends to occur in younger patients and at lower dosages of steroid therapy than seen with other associated diseases. Radiographic and CT findings progress from patchy sclerosis to a crescentic subchondral lucency, to fragmentation and collapse at the articular surface (Fig 22). MR imaging findings are more sensitive than CT findings and include the pathognomonic double-line sign on MR images obtained with fluid-sensitive sequences; this sign appears at the interface with infarcted bone as a hypointense peripheral line surrounding a more hyperintense inner line.

Osteomyelitis or Abscess.—Infectious complications are more common in the setting of Crohn disease secondary to transmural bowel inflammation and fistula formation (Fig 23). Retroperitoneal fistulas can result in iliopsoas or presacral abscesses (88). Although rare, osteomyelitis of the pelvic bones and spine can occur by way of fistulization or spread of a local abscess, with involvement of the iliac bones and sacrum most common, followed by the lumbar vertebrae, femoral heads, and hip joints (88).

Hypertrophic Osteoarthropathy.—IBD is a rare cause of secondary hypertrophic osteoarthropathy, which manifests as periosteal new bone formation, digital clubbing, and joint pain (Fig 24). The pathogenesis is thought to involve increased levels of prostaglandin E_2, platelet-derived growth factor, and vascular endothelial growth factor (89). Hypertrophic osteoarthropathy is highly associated with malignancy, especially lung cancer.

Pulmonary Manifestations of IBD

In their review of population studies, Black et al (90) found that IBD patients experience pulmonary symptoms with greater frequency than the general population. In a 10-year retrospective analysis, Raj et al (91) found a fourfold increased prevalence of IBD in their cohort of patients with airways disease. The prevalence of pulmonary manifestations of disease is highly variable, and the spectrum of manifestations is broad. The pathogenesis of IBD-related pulmonary findings is unknown but may relate to a common embryologic origin of respiratory and intestinal mucosa, a response to common antigen exposure of the lungs and intestinal epithelium, and/or a response to inflammatory

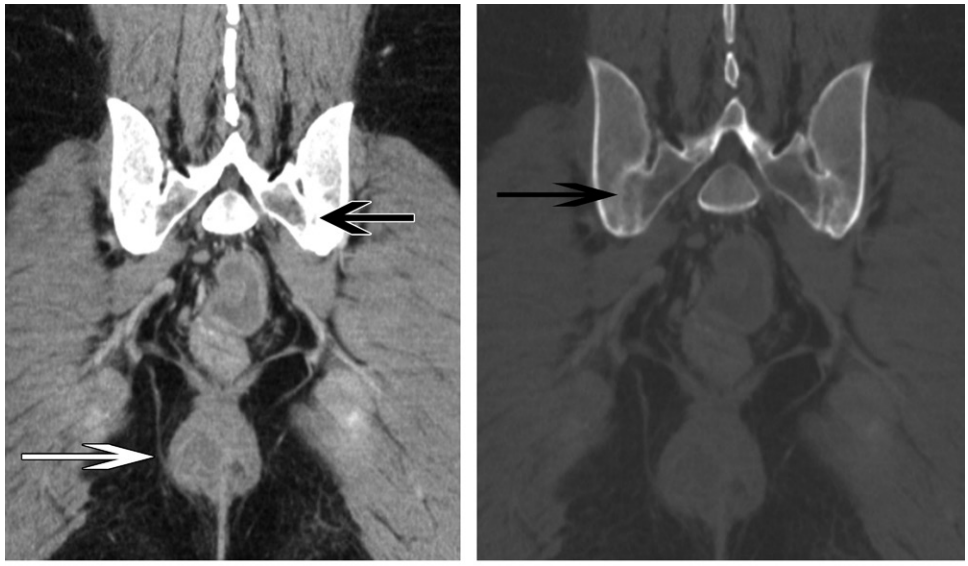

a. b.

Figure 23. Sacroiliitis and perirectal abscess in a 29-year-old man with Crohn disease. **(a)** Coronal CT image shows a perirectal abscess (white arrow), with partial ankylosis of the sacroiliac joints (black arrow). **(b)** Coronal CT image (bone window) better depicts the blurring of the joint space with erosive change and partial ankylosis (arrow).

a. b.

Figure 24. Hypertrophic osteoarthropathy in a 38-year-old man with nonspecific IBD who had left knee pain. **(a)** Anteroposterior radiograph of the left knee shows smooth linear periosteal reaction involving the long bones (arrows). The right knee (not shown) had similar findings. **(b)** Left to right: Anteroposterior, posteroanterior, and enlarged posteroanterior images from bone scan obtained with technetium Tc99m medronate show symmetric linear uptake along the cortical bone of the long bones (arrows), findings consistent with hypertrophic osteoarthropathy. Most cases of hypertrophic osteoarthropathy are secondary to thoracic or gastrointestinal disease. Although non–small cell lung cancer is the most common cause, IBD is a known gastrointestinal cause.

mediators released by the bowel (92). As knowledge of the genetic basis of IBD has grown, so has the appreciation of epidemiologic overlap of IBD with other immune-related inflammatory conditions that have pulmonary or airways involvement, including asthma, sarcoidosis (Fig 25), systemic lupus erythematosus, and rheumatoid arthritis (2). At times, it may be difficult or impossible to distinguish between processes that are primarily associated with IBD and the manifestations that occur in relation to treatment. Although respiratory manifestations most often follow a diagnosis of IBD, they may manifest months or years earlier in up to 10% of patients and may develop or worsen after colectomy

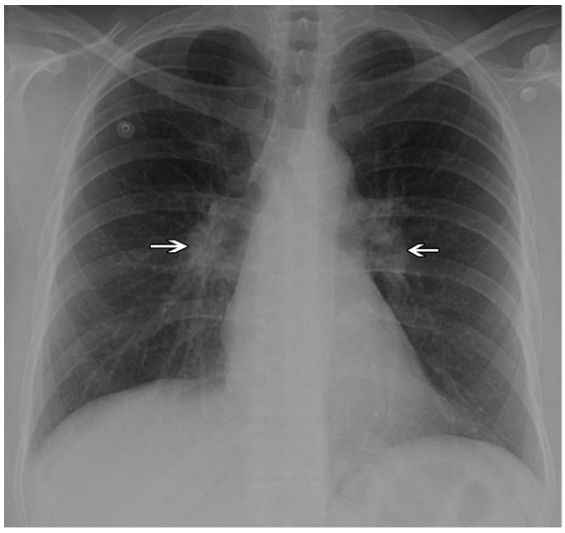

a.

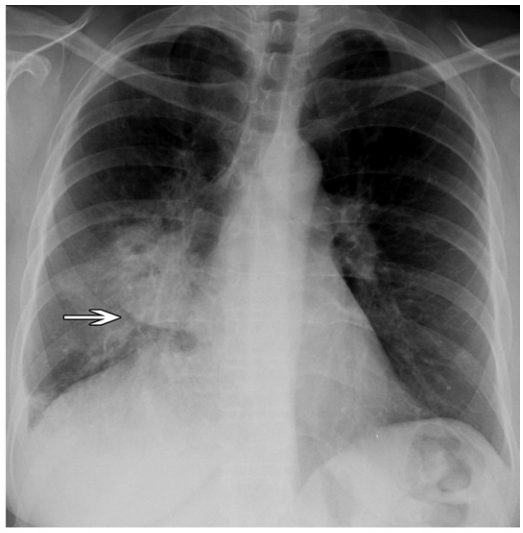

b.

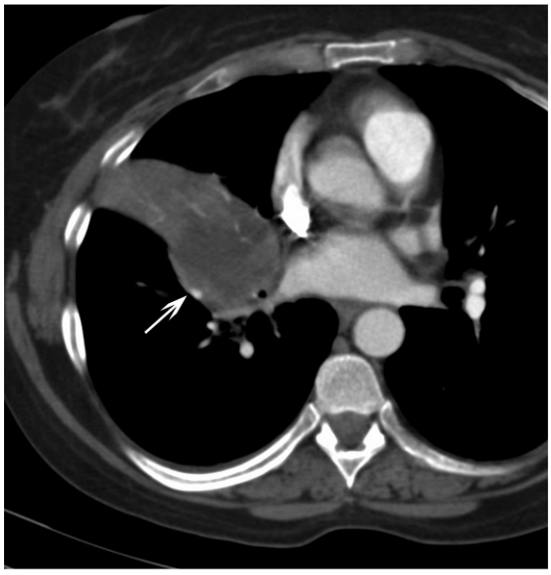

c.

Figure 25. IBD with sarcoidosis and treatment-related thoracic complications in a 54-year-old woman with Crohn disease. **(a)** Posteroanterior chest radiograph shows symmetric bilateral hilar fullness (arrows), a finding consistent with adenopathy. A skin rash was also present, and the histopathologic findings at examination of the specimen from bone biopsy were consistent with sarcoidosis. **(b)** Posteroanterior radiograph obtained 3 years after the image in **a**, when the patient presented with progressive respiratory symptoms, shows a focal right infrahilar opacity (arrow) with volume loss. **(c)** Corresponding axial contrast-enhanced CT image shows a low-attenuation right hilar mass (arrow), with postobstructive right middle lobe atelectasis. The findings at histopathologic examination of the specimen from endobronchial biopsy disclosed large B cells, and the patient tested positive for Epstein-Barr virus, findings consistent with a lymphoproliferative disorder attributable to treatment with 6-mercaptopurine.

in patients with ulcerative colitis (93). Respiratory system manifestations may involve the airways, lung parenchyma, vasculature, and serosa.

Large airways are the most common site of pulmonary involvement in patients with IBD (Fig 26), and such involvement has a stronger association with ulcerative colitis than with Crohn disease (90). Bronchiectasis is the most frequently reported airway manifestation, accounting for 66% of IBD-related large airway involvement, followed by chronic bronchitis. Suppurative airways disease without bronchiectasis and stenosis are less common. Imaging may show bronchial wall thickening and bronchiectasis, with or without mucoid impaction (94). Upper airway involvement and small airway involvement may be present but are far less common.

Lung parenchymal involvement is most commonly due to infection (Fig 27), whether community-acquired or related to treatment-associated immune suppression (95). In the results of a large retrospective cohort study, IBD patients had an 82% increased incidence of pneumonia compared with matched controls, and corticosteroid treatment was described as the strongest independent risk factor (96). Organizing pneumonia is the most common noninfectious IBD-related lung parenchymal manifestation (90,94). The true prevalence of organizing pneumonia as a primary manifestation of IBD is unknown, because the organizing pneumonia pattern of lung injury can be secondary to infection or drug toxicity. Imaging findings include multifocal patchy consolidation or ground-glass opacity with a subpleural or bronchovascular and mid to lower lung predominant distribution. Necrobiotic lung nodules that pathologically resemble those in rheumatoid arthritis (lung) and pyoderma gangrenosum (skin) have been described but are rare. Other uncommon IBD-related parenchymal manifestations include eosinophilic pneumonia (often associated with sulfasalazine therapy) and nonspecific interstitial pneumonia.

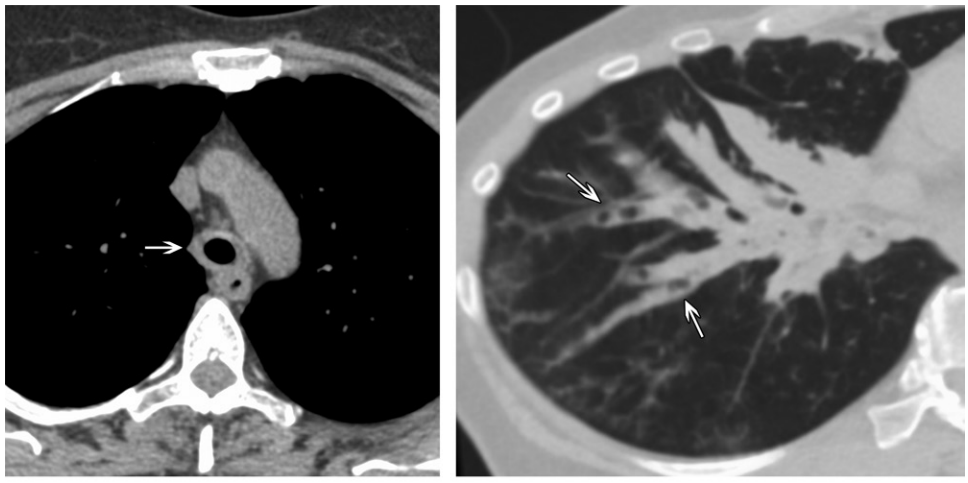

a. b.

Figure 26. Abnormalities of the large and medium airways in a 49-year-old woman with ulcerative colitis. **(a)** Axial CT image shows circumferential tracheal wall thickening (arrow). **(b)** Oblique volume-rendered CT image shows bronchiectasis and the debris material–filled airways of the right lower lobe (arrows), as well as right middle lobe atelectasis. Similar but less severe airway abnormalities were present in the lingula (not shown). (Case courtesy of Jonathan H. Chung, MD, University of Chicago, Chicago Ill.)

Serosal involvement can involve the pleura or pericardium. If pleural effusions are present, they are usually unilateral and exudative (90).

Venous thromboembolism is the most common and potentially life-threatening pulmonary vascular manifestation in patients with IBD. In the results of a recent meta-analysis of 11 studies, the IBD diagnosis conferred an increased relative risk of 2.2 (95% confidence interval: 1.83–2.65) for venous thromboembolism (97). Risk may be further increased during the systemic inflammation of an IBD flare.

Cardiac Manifestations of IBD

The relationship between IBD and cardiovascular disease has not been fully elucidated to date. In the findings from a number of meta-analyses and cohort studies in recent years, investigators have suggested that IBD patients have an increased risk of myocardial infarction, stroke, and cardiovascular mortality, particularly during periods of active bowel disease (98). The results of a recent Danish study showed an increased incidence of heart failure in IBD patients that strongly correlated with periods of active bowel disease (99). However, other investigators have suggested that there is no link between IBD and an increased incidence of cardiovascular disease. The results of a meta-analysis of 11 studies and 14 000 patients demonstrated no increase in cardiovascular mortality between the IBD group and the control group (95). Although the link between IBD and cardiovascular disease is not well established, most investigators agree that optimal treatment of IBD may prevent adverse cardiovascular events.

Ocular or Orbital Manifestations of IBD

In the results of population studies, investigators have estimated that the prevalence of ocular extraintestinal manifestations in the setting of IBD is between 4% and 12% (100). Ocular manifestations are more common in the setting of colonic IBD involvement, with a hypothesized shared pathogenesis involving immune complex–mediated hypersensitivity reactions (66). The most common ocular findings are not evaluated with imaging and include inflammatory conditions affecting different areas of the globe, ranging from conjunctivitis and episcleritis to more serious conditions such as scleritis and anterior uveitis (101). With scleritis or anterior uveitis, vision can be permanently impaired.

Although rare, orbital extraintestinal manifestations of IBD may be detected with imaging (92). Idiopathic orbital inflammation (pseudotumor) refers to inflammation of orbital structures, with imaging findings including masslike soft-tissue enhancement involving the tendinous insertions of the extraocular muscles, lacrimal gland, orbital fat, retrobulbar orbit, and the optic sheath. The prevalence of orbital pseudotumor in patients with IBD is not clear, but the findings from case reports suggest an association with Crohn disease (92). Optic nerve abnormalities in IBD are multifactorial and can occur secondary to optic neuritis, ischemia, treatment complications, and intracranial hypertension. Intracranial hypertension may be related to treatment or may be secondary to hypercoagulability and venous thrombosis (92). Additional reported orbital manifestations include orbital myositis and dacryoadenitis.

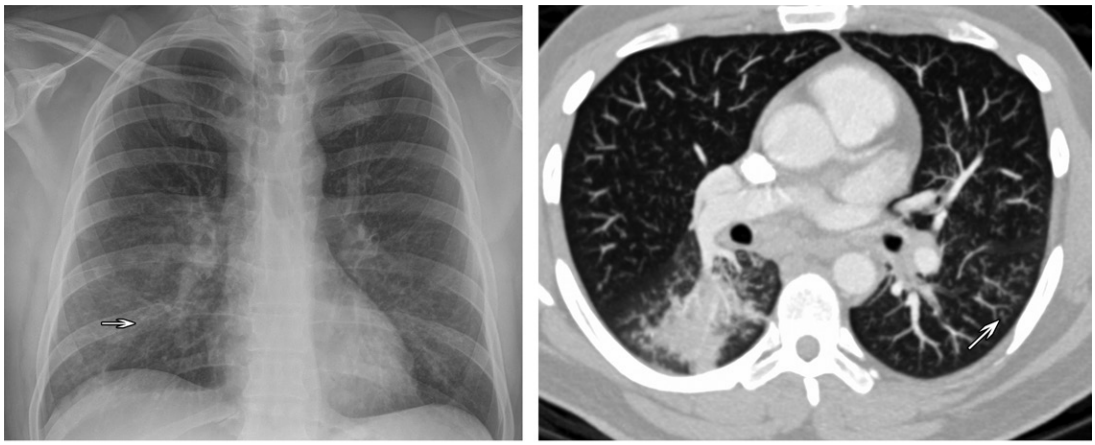

a. b.

Figure 27. Parenchymal consolidation in a 46-year-old man with ulcerative colitis who presented with increased sputum production and fever for the preceding 10 days. **(a)** Posteroanterior chest radiograph shows a subtle patchy opacity (arrow) in the right lower lung, along with occasionally thickened central airways, which were greater on the right than the left. **(b)** Contrast-enhanced axial maximum intensity projection CT image shows consolidation in the superior segment of the right lower lobe and centrilobular nodules (arrow) in the left lower lobe. The results of blood and sputum cultures were unrevealing. The patient was treated for a community-acquired lower respiratory tract infection and pneumonia, and his condition improved clinically. Infection is more common in IBD patients compared with the general population.

Figure 28. Perirectal fistula with perineal extension in a 40-year-old man with chronic Crohn disease. Sagittal T2-weighted MR image shows a diffuse inflammation of the rectum with a perirectal fistula (black arrow) extending inferiorly to the perineum (*). The findings at clinical examination disclosed active cutaneous drainage from the perineum, a finding that is also apparent on this MR image (white arrow).

Cutaneous Manifestations of IBD

Mucocutaneous manifestations are frequent extraintestinal manifestations, occurring in 22%–75% of patients with Crohn disease and in 5%–11% of patients with ulcerative colitis (102). Approximately 10% of patients with IBD demonstrate cutaneous manifestations at the time of diagnosis, with a variety of lesions occurring during the course of IBD (103). Cutaneous manifestations associated with IBD can be classified on the basis of their pathophysiologic mechanisms into four categories: *(a)* specific cutaneous manifestations with the same histologic features as IBD; *(b)* reactive cutaneous manifestations with shared pathophysiologic mechanisms; *(c)* skin diseases associated with IBD; and *(d)* manifestations from adverse effects of therapy for IBD.

Specific cutaneous manifestations demonstrate the same histopathologic features as the underlying bowel disease and occur only in Crohn disease, because ulcerative colitis does not extend to external mucosal membranes (102). Continuous or contiguous Crohn disease is the most common overall cutaneous feature in patients with IBD, occurring in up to 25%–80% of patients with Crohn disease (102), and includes perianal inflammation, enterocutaneous fistulas, fissures, ulcers, and abscesses. Radiologists can play an important role in the identification of fistulas and abscesses and their treatment planning. For example, MR imaging is increasingly recognized as an important technique for perianal fistula grading and surgical planning because of the ability of MR imaging to demonstrate hidden areas of infection and fistula extension that contribute to a high rate of recurrence (104). Active fistulous tracts appear most conspicuous on T2-weighted MR images, with hyperintense fluid in the tract and hypointense fibrous tissue in the fistula wall (Fig 28). Chronic fistulous tracts demonstrate low signal intensity on T1- and T2-weighted MR images. Contrast-enhanced fat-suppressed T1-weighted images will demonstrate intense enhancement of the active granulation tissue, while the fluid in the tract remains hypointense.

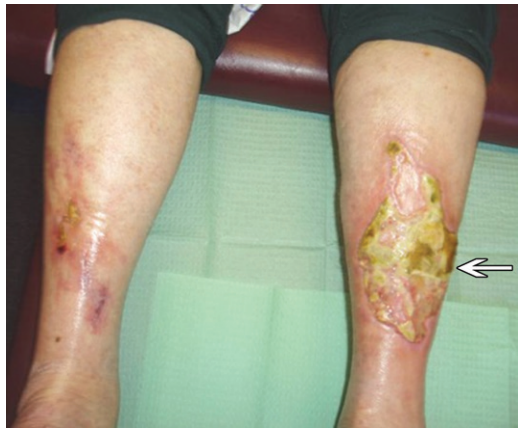

Figure 29. Pyoderma gangrenosum in a 55-year-old woman with nonspecific IBD. Photograph shows a broad ulcer (arrow) on the anterolateral portion of the left calf that is in the process of healing. The yellow-white tissue is due to cutaneous necrosis. The red papules and plaques are granulation tissue formed as the ulcer heals. This centripetal healing ("secondary intention") is slow, generally requiring months to fully heal. (Courtesy of John L. Bezzant, MD, Department of Dermatology, University of Utah, Salt Lake City, Utah.)

Reactive manifestations occur in both patients with ulcerative colitis and patients with Crohn disease. Reactive manifestations have separate pathologic features from those of IBD but share a pathophysiologic link related to innate immunity. Pyoderma gangrenosum is the most common reactive manifestation, occurring in 5%–20% of patients with ulcerative colitis and in 1%–2% of patients with Crohn disease (Fig 29) (102). Pyoderma gangrenosum can be severe and debilitating, often manifesting near the time of a bowel exacerbation. Pyoderma gangrenosum appears as a pustule or erythematous papule or nodule that rapidly ulcerates, forming a painful ulcer with violaceous, sharp undermined borders and a necrotic base. Pyoderma gangrenosum can be solitary or multifocal and most commonly develops on the extensor surface of the legs but can appear anywhere on the skin.

Erythema nodosum is the most common cutaneous manifestation associated with IBD, affecting 3%–10% of patients with ulcerative colitis and 4%–15% of patients with Crohn disease (102), and is commonly seen in women aged 25–40 years. Erythema nodosum in the setting of ulcerative colitis often occurs during active colitis, and erythema nodosum in the setting of Crohn disease is associated with colonic involvement. Lesions of erythema nodosum manifest as deep, tender, painful bluish-red nodules, which are most commonly symmetric, in the pretibial lower extremities. Lesions range in size from 1 to 5 cm, do not ulcerate, and typically heal within several weeks. Recurrence is common. Another associated cutaneous manifestation is psoriasis, which occurs in 7%–11% of patients with IBD (102) and follows a course independent of IBD activity.

Conclusion

Imaging of patients with IBD is being performed with ever greater frequency, both in academic centers and in private practice groups. Both CT enterography and MR enterography have evolved in recent years as robust methods in the detection and surveillance of IBD. Although cross-sectional enterography is primarily designed to evaluate the gastrointestinal tract, important extraintestinal conditions and complications of IBD may be recognized with such examinations. Increasing evidence suggests that IBD and associated extraintestinal disorders are not isolated diseases but share common mechanistic and pathophysiologic pathways, many of which remain elusive to date. IBD and associated disorders are complex disease entities that demand an interdisciplinary approach among various subspecialties, including gastroenterology and various surgical services. Radiologists involved in the interpretation of these imaging examinations must be aware of the extraintestinal manifestations of IBD to optimize clinical management of these complex patients.

References

1. Navaneethan U, Shen B. Hepatopancreatobiliary manifestations and complications associated with inflammatory bowel disease. Inflamm Bowel Dis 2010;16(9):1598–1619.
2. Lees CW, Barrett JC, Parkes M, Satsangi J. New IBD genetics: common pathways with other diseases. Gut 2011;60(12):1739–1753.
3. Bernstein CN, Blanchard JF, Rawsthorne P, Yu N. The prevalence of extraintestinal diseases in inflammatory bowel disease: a population-based study. Am J Gastroenterol 2001;96(4):1116–1122.
4. Smith MP, Loe RH. Sclerosing cholangitis: review of recent case reports and associated diseases and four new cases. Am J Surg 1965;110:239–246.
5. Lee YM, Kaplan MM. Primary sclerosing cholangitis. N Engl J Med 1995;332(14):924–933.
6. Broomé U, Bergquist A. Primary sclerosing cholangitis, inflammatory bowel disease, and colon cancer. Semin Liver Dis 2006;26(1):31–41.
7. Olsson R, Danielsson A, Järnerot G, et al. Prevalence of primary sclerosing cholangitis in patients with ulcerative colitis. Gastroenterology 1991;100(5 pt 1):1319–1323.
8. Loftus EV Jr, Harewood GC, Loftus CG, et al. PSC-IBD: a unique form of inflammatory bowel disease associated with primary sclerosing cholangitis. Gut 2005;54(1):91–96.
9. Joo M, Abreu-e-Lima P, Farraye F, et al. Pathologic features of ulcerative colitis in patients with primary sclerosing cholangitis: a case-control study. Am J Surg Pathol 2009;33(6):854–862.
10. Soetikno RM, Lin OS, Heidenreich PA, Young HS, Blackstone MO. Increased risk of colorectal neoplasia in patients with primary sclerosing cholangitis and ulcerative colitis: a meta-analysis. Gastrointest Endosc 2002;56(1):48–54.

11. Saarinen S, Olerup O, Broomé U. Increased frequency of autoimmune diseases in patients with primary sclerosing cholangitis. Am J Gastroenterol 2000;95(11):3195–3199.
12. Aoki CA, Bowlus CL, Gershwin ME. The immunobiology of primary sclerosing cholangitis. Autoimmun Rev 2005;4(3):137–143.
13. Terjung B, Spengler U. Atypical p-ANCA in PSC and AIH: a hint toward a "leaky gut"? Clin Rev Allergy Immunol 2009;36(1):40–51.
14. Tischendorf JJ, Hecker H, Krüger M, Manns MP, Meier PN. Characterization, outcome, and prognosis in 273 patients with primary sclerosing cholangitis: a single center study. Am J Gastroenterol 2007;102(1):107–114.
15. Berstad AE, Aabakken L, Smith HJ, Aasen S, Boberg KM, Schrumpf E. Diagnostic accuracy of magnetic resonance and endoscopic retrograde cholangiography in primary sclerosing cholangitis. Clin Gastroenterol Hepatol 2006;4(4):514–520.
16. Floreani A, Rizzotto ER, Ferrara F, et al. Clinical course and outcome of autoimmune hepatitis/primary sclerosing cholangitis overlap syndrome. Am J Gastroenterol 2005;100(7):1516–1522.
17. Gregorio GV, Portmann B, Karani J, et al. Autoimmune hepatitis/sclerosing cholangitis overlap syndrome in childhood: a 16-year prospective study. Hepatology 2001;33(3):544–553.
18. Sahni VA, Raghunathan G, Mearadji B, et al. Autoimmune hepatitis: CT and MR imaging features with histopathological correlation. Abdom Imaging 2010;35(1):75–84.
19. Chung YE, Kim MJ, Park YN, et al. Varying appearances of cholangiocarcinoma: radiologic-pathologic correlation. RadioGraphics 2009;29(3):683–700.
20. Broomé U, Olsson R, Lööf L, et al. Natural history and prognostic factors in 305 Swedish patients with primary sclerosing cholangitis. Gut 1996;38(4):610–615.
21. Walker SL, McCormick PA. Diagnosing cholangiocarcinoma in primary sclerosing cholangitis: an "evidence based radiology" review. Abdom Imaging 2008;33(1):14–17.
22. Choi JY, Kim MJ, Lee JM, et al. Hilar cholangiocarcinoma: role of preoperative imaging with sonography, MDCT, MRI, and direct cholangiography. AJR Am J Roentgenol 2008;191(5):1448–1457.
23. Roenigk HH Jr, Auerbach R, Maibach H, Weinstein G, Lebwohl M. Methotrexate in psoriasis: consensus conference. J Am Acad Dermatol 1998;38(3):478–485.
24. Mortele KJ, Ros PR. Imaging of diffuse liver disease. Semin Liver Dis 2001;21(2):195–212.
25. Kurtz AB, Rubin CS, Cooper HS, et al. Ultrasound findings in hepatitis. Radiology 1980;136(3):717–723.
26. Russmann S, Zimmermann A, Krähenbühl S, Kern B, Reichen J. Veno-occlusive disease, nodular regenerative hyperplasia and hepatocellular carcinoma after azathioprine treatment in a patient with ulcerative colitis. Eur J Gastroenterol Hepatol 2001;13(3):287–290.
27. Restellini S, Chazouillères O, Frossard JL. Hepatic manifestations of inflammatory bowel diseases. Liver Int doi:10.1111/liv.13265. Published online October 6, 2016.
28. Bargiggia S, Maconi G, Elli M, et al. Sonographic prevalence of liver steatosis and biliary tract stones in patients with inflammatory bowel disease: study of 511 subjects at a single center. J Clin Gastroenterol 2003;36(5):417–420.
29. Riegler G, D'Incà R, Sturniolo GC, et al. Hepatobiliary alterations in patients with inflammatory bowel disease: a multicenter study—Caprilli & Gruppo Italiano Studio Colon-Retto. Scand J Gastroenterol 1998;33(1):93–98.
30. Ma X, Holalkere NS, Kambadakone RA, Mino-Kenudson M, Hahn PF, Sahani DV. Imaging-based quantification of hepatic fat: methods and clinical applications. RadioGraphics 2009;29(5):1253–1277.
31. Outwater EK, Blasbalg R, Siegelman ES, Vala M. Detection of lipid in abdominal tissues with opposed-phase gradient-echo images at 1.5 T: techniques and diagnostic importance. RadioGraphics 1998;18(6):1465–1480.
32. Vakil N, Hayne G, Sharma A, Hardy DJ, Slutsky A. Liver abscess in Crohn's disease. Am J Gastroenterol 1994;89(7):1090–1095.
33. Benedetti NJ, Desser TS, Jeffrey RB. Imaging of hepatic infections. Ultrasound Q 2008;24(4):267–278.
34. Alsaif HS, Venkatesh SK, Chan DS, Archuleta S. CT appearance of pyogenic liver abscesses caused by *Klebsiella pneumoniae*. Radiology 2011;260(1):129–138.
35. Jeffrey RB Jr, Tolentino CS, Chang FC, Federle MP. CT of small pyogenic hepatic abscesses: the cluster sign. AJR Am J Roentgenol 1988;151(3):487–489.
36. Miehsler W, Reinisch W, Valic E, et al. Is inflammatory bowel disease an independent and disease specific risk factor for thromboembolism? Gut 2004;53(4):542–548.
37. Jackson LM, O'Gorman PJ, O'Connell J, Cronin CC, Cotter KP, Shanahan F. Thrombosis in inflammatory bowel disease: clinical setting, procoagulant profile and factor V Leiden. QJM 1997;90(3):183–188.
38. Baker ME, Remzi F, Einstein D, et al. CT depiction of portal vein thrombi after creation of ileal pouch–anal anastomosis. Radiology 2003;227(1):73–79.
39. Hidajat N, Stobbe H, Griesshaber V, Felix R, Schroder RJ. Imaging and radiological interventions of portal vein thrombosis. Acta Radiol 2005;46(4):336–343.
40. Barthet M, Hastier P, Bernard JP, et al. Chronic pancreatitis and inflammatory bowel disease: true or coincidental association? Am J Gastroenterol 1999;94(8):2141–2148.
41. Katz S, Bank S, Greenberg RE, Lendvai S, Lesser M, Napolitano B. Hyperamylasemia in inflammatory bowel disease. J Clin Gastroenterol 1988;10(6):627–630.
42. Matsumoto T, Matsui T, Iida M, Nunoi K, Fujishima M. Acute pancreatitis as a complication of Crohn's disease. Am J Gastroenterol 1989;84(7):804–807.
43. Lankisch PG, Dröge M, Gottesleben F. Drug induced acute pancreatitis: incidence and severity. Gut 1995;37(4):565–567.
44. Kazumori H, Ashizawa N, Moriyama N, et al. Primary sclerosing pancreatitis and cholangitis. Int J Pancreatol 1998;24(2):123–127.
45. Sheu Y, Furlan A, Almusa O, Papachristou G, Bae KT. The revised Atlanta classification for acute pancreatitis: a CT imaging guide for radiologists. Emerg Radiol 2012;19(3):237–243.
46. Baker ME, Nelson RC, Rosen MP, et al. ACR Appropriateness Criteria® acute pancreatitis. Ultrasound Q 2014;30(4):267–273.
47. Ball WP, Baggenstoss AH, Bargen JA. Pancreatic lesions associated with chronic ulcerative colitis. Arch Pathol (Chic) 1950;50(3):347–358.
48. Chapin LE, Scudamore HH, Baggenstoss AH, Bargen JA. Regional enteritis: associated visceral changes. Gastroenterology 1956;30(3):404–415.
49. Stöcker W, Otte M, Ulrich S, et al. Autoimmunity to pancreatic juice in Crohn's disease: results of an autoantibody screening in patients with chronic inflammatory bowel disease. Scand J Gastroenterol Suppl 1987;139:41–52.
50. Remer EM, Baker ME. Imaging of chronic pancreatitis. Radiol Clin North Am 2002;40(6):1229–1242, v.
51. Manikkavasakar S, AlObaidy M, Busireddy KK, et al. Magnetic resonance imaging of pancreatitis: an update. World J Gastroenterol 2014;20(40):14760–14777.
52. Dastis SN, Latinne D, Sempoux C, Geubel AP. Ulcerative colitis associated with IgG4 cholangitis: similar features in two HLA identical siblings. J Hepatol 2009;51(3):601–605.
53. Tada F, Abe M, Nunoi H, et al. Ulcerative colitis complicated with primary biliary cirrhosis. Intern Med 2011;50(20):2323–2327.
54. Wenzel JS, Donohoe A, Ford KL 3rd, Glastad K, Watkins D, Molmenti E. Primary biliary cirrhosis: MR imaging findings and description of MR imaging periportal halo sign. AJR Am J Roentgenol 2001;176(4):885–889.
55. Ravi K, Chari ST, Vege SS, Sandborn WJ, Smyrk TC, Loftus EV Jr. Inflammatory bowel disease in the setting of autoimmune pancreatitis. Inflamm Bowel Dis 2009;15(9):1326–1330.
56. Khandelwal A, Shanbhogue AK, Takahashi N, Sandrasegaran K, Prasad SR. Recent advances in the diagnosis and management of autoimmune pancreatitis. AJR Am J Roentgenol 2014;202(5):1007–1021.
57. Tonolini M, Villa C, Campari A, Ravelli A, Bianco R, Cornalba G. Common and unusual urogenital Crohn's disease complications: spectrum of cross-sectional imaging findings. Abdom Imaging 2013;38(1):32–41.
58. Talamini MA, Broe PJ, Cameron JL. Urinary fistulas in Crohn's disease. Surg Gynecol Obstet 1982;154(4):553–556.
59. Goldman SM, Fishman EK, Gatewood OM, Jones B, Siegelman SS. CT in the diagnosis of enterovesical fistulae. AJR Am J Roentgenol 1985;144(6):1229–1233.
60. Ruffolo C, Angriman I, Scarpa M, et al. Urologic complications in Crohn's disease: suspicion criteria. Hepatogastroenterology 2006;53(69):357–360.
61. McLeod RS, Churchill DN. Urolithiasis complicating inflammatory bowel disease. J Urol 1992;148(3 pt 2):974–978.
62. Pardi DS, Tremaine WJ, Sandborn WJ, McCarthy JT. Renal and urologic complications of inflammatory bowel disease. Am J Gastroenterol 1998;93(4):504–514.

63. Woolfson RG, Mansell MA. Hyperoxaluria and renal calculi. Postgrad Med J 1994;70(828):695–698.
64. National Guideline Clearinghouse. ACR Appropriateness Criteria®: acute onset flank pain—suspicion of stone disease (urolithiasis). National Guideline Clearinghouse website. https://www.guideline.gov/summaries/summary/49919/acr-appropriateness-criteria--acute-onset-flank-pain---suspicion-of-stone-disease-urolithiasis. Updated January 29, 2016.
65. Semins MJ, Feng Z, Trock B, Bohlman M, Hosek W, Matlaga BR. Evaluation of acute renal colic: a comparison of non-contrast CT versus 3-T non-contrast HASTE MR urography. Urolithiasis 2013;41(1):43–46.
66. Levine JS, Burakoff R. Extraintestinal manifestations of inflammatory bowel disease. Gastroenterol Hepatol (N Y) 2011;7(4):235–241.
67. Arvikar SL, Fisher MC. Inflammatory bowel disease associated arthropathy. Curr Rev Musculoskelet Med 2011;4(3):123–131.
68. Sheth T, Pitchumoni CS, Das KM. Musculoskeletal manifestations in inflammatory bowel disease: a revisit in search of immunopathophysiological mechanisms. J Clin Gastroenterol 2014;48(4):308–317.
69. Brakenhoff LK, van der Heijde DM, Hommes DW, Huizinga TW, Fidder HH. The joint-gut axis in inflammatory bowel diseases. J Crohn's Colitis 2010;4(3):257–268.
70. Mielants H, Veys EM, Cuvelier C, De Vos M. Subclinical involvement of the gut in undifferentiated spondylarthropathies. Clin Exp Rheumatol 1989;7(5):499–504.
71. Orchard TR, Wordsworth BP, Jewell DP. Peripheral arthropathies in inflammatory bowel disease: their articular distribution and natural history. Gut 1998;42(3):387–391.
72. Palm Ø, Moum B, Jahnsen J, Gran JT. The prevalence and incidence of peripheral arthritis in patients with inflammatory bowel disease: a prospective population-based study (the IBSEN study). Rheumatology (Oxford) 2001;40(11):1256–1261.
73. Sheth T, Pitchumoni CS, Das KM. Management of musculoskeletal manifestations in inflammatory bowel disease. Gastroenterol Res Pract 2015;2015:387891. doi:10.1155/2015/387891. Published online June 10, 2015.
74. Kataria RK, Brent LH. Spondyloarthropathies. Am Fam Physician 2004;69(12):2853–2860.
75. Bakewell CJ, Olivieri I, Aydin SZ, et al. Ultrasound and magnetic resonance imaging in the evaluation of psoriatic dactylitis: status and perspectives. J Rheumatol 2013;40(12):1951–1957.
76. Baeten D, De Keyser F, Mielants H, Veys EM. Ankylosing spondylitis and bowel disease. Best Pract Res Clin Rheumatol 2002;16(4):537–549.
77. van der Linden S, Valkenburg HA, Cats A. Evaluation of diagnostic criteria for ankylosing spondylitis: a proposal for modification of the New York criteria. Arthritis Rheum 1984;27(4):361–368.
78. Amor B, Dougados M, Mijiyawa M. Criteria of the classification of spondylarthropathies [in French]. Rev Rhum Mal Osteoartic 1990;57(2):85–89.
79. Dougados M, van der Linden S, Juhlin R, et al. The European Spondylarthropathy Study Group preliminary criteria for the classification of spondylarthropathy. Arthritis Rheum 1991;34(10):1218–1227.
80. Navallas M, Ares J, Beltrán B, Lisbona MP, Maymó J, Solano A. Sacroiliitis associated with axial spondyloarthropathy: new concepts and latest trends. RadioGraphics 2013;33(4):933–956.
81. Battistone MJ, Manaster BJ, Reda DJ, Clegg DO. Radiographic diagnosis of sacroiliitis: are sacroiliac views really better? J Rheumatol 1998;25(12):2395–2401.
82. Rudwaleit M, Jurik AG, Hermann KG, et al. Defining active sacroiliitis on magnetic resonance imaging (MRI) for classification of axial spondyloarthritis: a consensual approach by the ASAS/OMERACT MRI group. Ann Rheum Dis 2009;68(10):1520–1527.
83. Stürzenbecher A, Braun J, Paris S, Biedermann T, Hamm B, Bollow M. MR imaging of septic sacroiliitis. Skeletal Radiol 2000;29(8):439–446.
84. Rudwaleit M, van der Heijde D, Landewé R, et al. The development of Assessment of SpondyloArthritis International Society classification criteria for axial spondyloarthritis (part II): validation and final selection. Ann Rheum Dis 2009;68(6):777–783.
85. Rudwaleit M, Baeten D. Ankylosing spondylitis and bowel disease. Best Pract Res Clin Rheumatol 2006;20(3):451–471.
86. Hermann KG, Althoff CE, Schneider U, et al. Spinal changes in patients with spondyloarthritis: comparison of MR imaging and radiographic appearances. RadioGraphics 2005;25(3):559–569; discussion 569–570.
87. Bernstein CN, Leslie WD, Leboff MS. AGA technical review on osteoporosis in gastrointestinal diseases. Gastroenterology 2003;124(3):795–841.
88. Tonolini M, Ravelli A, Campari A, Bianco R. Comprehensive MRI diagnosis of sacral osteomyelitis and multiple muscle abscesses as a rare complication of fistulizing Crohn's disease. J Crohn's Colitis 2011;5(5):473–476.
89. Rhee SM, Park KJ, Ha YC. Hypertrophic osteoarthropathy in patient with Crohn's disease: a case report. J Bone Metab 2014;21(2):151–154.
90. Black H, Mendoza M, Murin S. Thoracic manifestations of inflammatory bowel disease. Chest 2007;131(2):524–532.
91. Raj AA, Birring SS, Green R, Grant A, de Caestecker J, Pavord ID. Prevalence of inflammatory bowel disease in patients with airways disease. Respir Med 2008;102(5):780–785.
92. Katsanos A, Asproudis I, Katsanos KH, Dastiridou AI, Aspiotis M, Tsianos EV. Orbital and optic nerve complications of inflammatory bowel disease. J Crohn's Colitis 2013;7(9):683–693.
93. Camus P, Piard F, Ashcroft T, Gal AA, Colby TV. The lung in inflammatory bowel disease. Medicine (Baltimore) 1993;72(3):151–183.
94. Betancourt SL, Palacio D, Jimenez CA, Martinez S, Marom EM. Thoracic manifestations of inflammatory bowel disease. AJR Am J Roentgenol 2011;197(3):W452–W456.
95. Dorn SD, Sandler RS. Inflammatory bowel disease is not a risk factor for cardiovascular disease mortality: results from a systematic review and meta-analysis. Am J Gastroenterol 2007;102(3):662–667.
96. Long MD, Martin C, Sandler RS, Kappelman MD. Increased risk of pneumonia among patients with inflammatory bowel disease. Am J Gastroenterol 2013;108(2):240–248.
97. Yuhara H, Steinmaus C, Corley D, et al. Meta-analysis: the risk of venous thromboembolism in patients with inflammatory bowel disease. Aliment Pharmacol Ther 2013;37(10):953–962.
98. Kristensen SL, Ahlehoff O, Lindhardsen J, et al. Disease activity in inflammatory bowel disease is associated with increased risk of myocardial infarction, stroke and cardiovascular death: a Danish nationwide cohort study. PLoS One 2013;8(2):e56944. doi:10.1371/journal.pone.0056944. Published online February 15, 2013. [Published correction appears in PLoS One 2013;8(4). doi:10.1371/annotation/b4a49855-87b9-436a-a4bd-bc64b50a6c93.]
99. Kristensen SL, Ahlehoff O, Lindhardsen J, et al. Inflammatory bowel disease is associated with an increased risk of hospitalization for heart failure: a Danish Nationwide Cohort study. Circ Heart Fail 2014;7(5):717–722.
100. Das KM. Relationship of extraintestinal involvements in inflammatory bowel disease: new insights into autoimmune pathogenesis. Dig Dis Sci 1999;44(1):1–13.
101. Rothfuss KS, Stange EF, Herrlinger KR. Extraintestinal manifestations and complications in inflammatory bowel diseases. World J Gastroenterol 2006;12(30):4819–4831.
102. Marzano AV, Borghi A, Stadnicki A, Crosti C, Cugno M. Cutaneous manifestations in patients with inflammatory bowel diseases: pathophysiology, clinical features, and therapy. Inflamm Bowel Dis 2014;20(1):213–227.
103. Tavarela Veloso F. Review article: skin complications associated with inflammatory bowel disease. Aliment Pharmacol Ther 2004;20(suppl 4):50–53.
104. de Miguel Criado J, del Salto LG, Rivas PF, et al. MR imaging evaluation of perianal fistulas: spectrum of imaging features. RadioGraphics 2012;32(1):175–194.